



HAL
open science

The tectono-magmatic and subsidence evolution during lithospheric breakup in a salt-rich rifted margin: Insights from a 3D seismic survey from southern Gabon

Marie-Eva Epin, Gianreto Manatschal, François Sapin, Mark Rowan

► To cite this version:

Marie-Eva Epin, Gianreto Manatschal, François Sapin, Mark Rowan. The tectono-magmatic and subsidence evolution during lithospheric breakup in a salt-rich rifted margin: Insights from a 3D seismic survey from southern Gabon. *Marine and Petroleum Geology*, 2021, 128, pp.105005. 10.1016/j.marpetgeo.2021.105005 . hal-03514410

HAL Id: hal-03514410

<https://hal.science/hal-03514410>

Submitted on 22 Mar 2023

HAL is a multi-disciplinary open access archive for the deposit and dissemination of scientific research documents, whether they are published or not. The documents may come from teaching and research institutions in France or abroad, or from public or private research centers.

L'archive ouverte pluridisciplinaire **HAL**, est destinée au dépôt et à la diffusion de documents scientifiques de niveau recherche, publiés ou non, émanant des établissements d'enseignement et de recherche français ou étrangers, des laboratoires publics ou privés.



Distributed under a Creative Commons Attribution - NonCommercial 4.0 International License

The tectono-magmatic and subsidence evolution during lithospheric breakup in a salt-rich rifted margin: insights from a 3D seismic survey from southern Gabon

Marie-Eva Epin¹ (meepin@unistra.fr), Gianreto Manatschal¹, François Sapin², Mark G. Rowan³

1 : Institut Terre et Environnement de Strasbourg; UMR 7063, Université de Strasbourg/EOST, CNRS; 1 rue Blessig, F-67084 Strasbourg Cedex, France

2 : Total Pau, Centre Scientifique et Technique Jean Feger, Avenue Larribau F-64018, Pau, France

3 : Rowan Consulting, Inc., 850 8th St., Boulder, CO 80302, USA

Abstract

In this study, we present an interpretation of a 3D depth-migrated dataset imaging the Ocean Continent-Transition (OCT) of the southern Gabon margin. Located in an area where salt is not strongly overflowing the OCT, it allows the geometrical relationships of salt deposition and its relative timing to breakup to be determined. The OCT is formed by extensional propagators floored by exhumed mantle limited by either fault-bounded upper-crustal or pre-salt sediments and/or magmatic additions. Based on our interpretations, we conclude that the pre-salt sequence was deposited over a wide area spanning crustal thinning to the onset of hyperextension and exhumation. The relative timing of salt deposition is constrained by the observations that detachment faults break away in the pre-salt sequence and that some of these faults also strongly offset the base salt and are linked to the creation of accommodation space in the salt. This is direct proof that salt was deposited during mantle exhumation. Salt deposition is interpreted to have occurred at variable depths. Evaporites formed approximately 1 km below sea level in the north, above a 4 to 6 km thick pre-salt sequence, and as deep as 2 km in the south. In this area, salt is interpreted to directly overlie exhumed mantle, but whether it was deposited on mantle or juxtaposed during exhumation remains more debatable. Space created in the faulted outer trough was filled partly by autochthonous salt and possibly also by downslope flow. Rifting continued after the cessation of salt deposition, followed by magmatic additions in the outer high and ultimately the onset of seafloor spreading and the formation of Penrose oceanic crust.

Key words: Ocean-continent transition, break-up, subsidence, salt, exhumed mantle, failed rift axis

1. Introduction

Understanding how, where and when continental lithospheric plates rupture and new oceanic crust forms remains challenging because the sites where plates broke are in deep-water domains and often buried by thick post-rift sediments. At present, such domains have been imaged only in few places by high-quality 2D or 3D seismic surveys. Key questions are how extensional and magmatic processes interact during breakup, how these processes are documented in the crustal architecture and stratigraphic record and what is the depositional relief linked to the process of breakup. We try to answer these questions using high-quality seismic reflection data from a 3D seismic block, located in the southern distal Gabon margin that images the Ocean-Continent-Transition (OCT) down to 20 km depth. The OCT is here defined as the domain between hyperextended continental crust and oceanic crust. The study area is unique in the sense that this is one of the few areas in the Central segment of the South Atlantic where the OCT is locally not masked by salt. This, in combination with the quality of the seismic images, enables us to get unprecedented access to the structure of the OCT, to describe the relations between crustal thinning, magmatic addition and sedimentation, including salt deposition, and to discuss the tectonic and isostatic evolution of lithospheric breakup.

Although in the last decade a lot of new observations and concepts have been developed on distal rifted margins, the transition between the distal and oceanic domains remains poorly documented. Significant progress has been made in areas where good seismic data exist (e.g. Gulf of Guinea (Gillard et al., 2017); the conjugate Australia-Antarctica margin (Gillard et al., 2015); the South China Sea (Ding et al., 2016; Larsen et al., 2018; Nirrengarten et al., 2020); the North Atlantic (Péron-Pinvidic & Osmundsen, 2016); or the Austral segment of the South Atlantic (Clerc et al., 2018; Chauvet et al., 2020). However, only in few locations has the OCT been either drilled (Iberia-Newfoundland margins (DSDP Leg 11, ODP Legs 103, 149, 173, 210) and South China Sea (IODP Expeditions 367 & 368)) or dredged (southwestern Australia margin (Beslier et al., 2004) and

northwestern Iberia margin (Charpentier et al., 1998). The few examples show that breakup resulted from the interaction of igneous and extensional processes. However, the budget and timing of magma, the amount of extension and the resulting structure of the OCT can be variable not only from one margin to the other, but even along the same margin. Therefore, future work is needed to describe in more detail the along-strike architecture of OCTs at distal rifted margins. High resolution 3D seismic surveys of OCTs have so far been published only from the Iberian margin (Lymer et al., 2019). However, this study did not image the transition from extended crust to first oceanic crust. As a consequence, questions remain to be answered, such as: where does unequivocal continental crust finish and oceanic crust start? How can the zone where this transition occurs be defined and was exhumed mantle involved in its formation? What is the relationship between extended crust and new magmatic crust? And what is the link to the sediments and in particular to salt deposition and deformation in these domains? Some of these questions have been discussed in recent papers dealing with the Central segment of the South Atlantic (Dupré et al., 2007; Davison, 2007; Norton et al., 2016; Clerc et al., 2018; Rowan, 2018; Lavier et al., 2019; Fernandez et al., 2020; Chauvet et al., 2020) or the Gulf of Mexico (Pindell et al., 2014, 2018; Rowan, 2018; Hudec et al., 2020) which is a similar late syn-rift salt basin.

In this study we describe and interpret three dip seismic profiles and one strike seismic profile from a 3D seismic survey imaging down to 20 km depth from the distal southern Gabon margin (Fig. 1a; Duval & Firth, 2015). We focus on the along-strike variation of the OCT. The aims of this study are threefold: 1) to describe the 3D crustal architecture of the OCT, including the salt, using sections and maps; 2) to discuss the processes controlling the transition from rifting to seafloor spreading; and 3) to investigate under what paleogeographical conditions breakup may have occurred, including the relative timing and spatial distribution of evaporite deposition in the final margin architecture.

2. Geological setting

2.1. The South Atlantic

The South Atlantic can be subdivided into the Equatorial, Central and Austral segments (Moulin et al., 2005). These segments formed during diachronous, northward propagating rifting and resulted in

the breakup of Gondwana from late Jurassic-Neocomian (Austral segment) to the Albian (Equatorial segment) (Mounguengui & Guiraud, 2009, Davison, 1999). The detailed temporal and spatial evolution of breakup is, however, debated as indicated by conflicting plate kinematic reconstructions (e.g. Torsvik et al., 2009; Heine et al., 2013; Moulin et al., 2010 and references therein). Along-strike changes include the budget of magma (more magmatic in the Austral segment: Gladchenko et al., 1997; Stica et al., 2014); the occurrence of Aptian salt in the Central segment (Lentini et al., 2010, Norton et al., 2014, Rowan 2018) and the importance of segmentation and transform faulting in the Equatorial segment (Moulin et al., 2015). Within the Central segment discussed in this paper, the distribution of magma and salt is complex and influences the along-strike architecture of the margin. None of the archetype models of rifted margins can fully explain the evolution of the entire South Atlantic Central segment. This is due to the fact that the rift evolution, even within a segment, is controlled by several factors, including inheritance (Stanton et al., 2018), which can explain different rheologies (Clerc et al., 2018), magmatic budgets (Tugend et al., 2020) and along-strike changes in the rift asymmetry from lower- to upper-plate margins (Péron-Pinvidic et al., 2017).

2.2. The south Gabon margin

The south Gabon margin is located on the West African margin and belongs to the Central segment of the South Atlantic. The first rifting phase occurred during the Early Cretaceous (~144 Ma, Neocomian-Berriasian to ~127 Ma, Middle Barremian) resulting in a mega-sequence consisting predominantly of sediments deposited in continental environments (Guiraud & Maurin, 1991). This early rift sequence is well exposed onshore in fault bounded rift basins. A second rift event resulted in the migration of extension basinward (i.e. seaward) and is associated with a thick sedimentary sequence, referred here to as the pre-salt sequence. The pre-salt sequence dated from Middle Barremian to Late Aptian (~127-113Ma) was deposited in fluvial to lacustrine and shallow-marine environments (e.g. Dental Fm., Fig. 1; Dupré et al., 2007). This thick pre-salt sequence formed during crustal thinning (~127-118 Ma; Mounguengui & Guiraud, 2009) and early hyperextension (Vembo-Gamba Fms, 116-113 Ma) and is overlain by thick evaporites deposited during the latest Aptian (113-112 Ma). The exact time and duration of evaporite deposition has not been established with confidence

since the more distal parts of the margin have not been drilled. This salt sequence was covered by carbonate platforms and distal equivalents in the earliest Albian (Dupré et al., 2007, Fig. 1c). Gravitational processes involving the Lower Albian sediments are documented from the Late Albian onwards. Based on the present-day structural configuration of the salt, the margin can be divided into three domains: the extensional and the contractional domains and a frontal allochthonous nappe. Above the supra-salt carbonates, further post-rift sediments were deposited in a predominantly deep-water, open-marine depositional environment. These Upper Cretaceous to Tertiary formations were mainly composed of siliciclastic turbidites with mudstone, sandstone and occasional limestone beds. The post-rift sequence is characterized by major erosional unconformities during Tertiary time (Dupré et al., 2007).

Representative seismic lines across the west African salt-bearing margin, imaging the whole margin architecture, have been published by Péron Pinvidic et al. (2017) and Clerc et al. (2018). Both sections show evidence for hyperextension, but the interpretations of the style and the detailed architecture of the most distal parts of the margin are different. In Fig. 1b we show the large-scale interpretation of a line across the northern Angolan margin published by Péron-Pinvidic et al. (2017). The position of the drill hole G2 (see Fig. 7c; described by Dupré et al., 2007) is shown in Fig. 1a. Although Fernandez et al. (2020) argue against mantle exhumation in this area, Péron-Pinvidic et al. (2017) interpret a hyperextended continental crust that wedges out and is separated by a domain of exhumed mantle from the first unequivocal oceanic crust. The most distal domain is overlain by syn-rift sediments, described in this paper as “pre-salt”, overlain by salt, the frontal portion of which is allochthonous. This classical description of a distal domain will be revised in this study in view of the new high-quality seismic imaging of this domain. We will describe in much more detail the domains separating the hyperextended crust and the first oceanic crust. The oceanic crust is believed to have been generated in the late Aptian (Meyers et al., 1996). However, its precise age is difficult to establish because: (i) the earliest oceanic crust formed during the Cretaceous magnetic quiet period, and (ii) basement rocks or syn-tectonic sequences in the OCT have not been drilled.

3. Data set and methods

3.1. Data set

This study is based on the interpretation of a 3D seismic survey of 25,000 km², acquired and provided by CGG Multi-Client and New Ventures (location on Fig. 1a). It is a large-scale multi-client seismic survey, during which marine magnetic and gravity data were acquired concurrently (Parsons et al., 2017). Data acquisition began in 2015 and was performed by two vessels, the *Geo Caribbean* and the *Oceanic Endeavour*, each towing 10 x 10 km streamers at 120 m separation (Duval & Firth, 2015). The final output Pre-Stack Depth Migration (PreSDM) extends to a depth of 20 km in order to enable imaging and modelling of deep crustal features (for more detail see Duval & Firth, 2015; Parsons et al., 2017; Duran et al., 2018).

3.2. Methods

In this study, the interpretation is entirely based on a new 3D seismic survey. The main aim of this paper is to unravel, based on the geometric relationships observed in the high-resolution seismic data, the architecture and time-space relationships observed in the OCT. Previous studies by Dupré et al. (2007) and Fernandez et al. (2020) used potential-field methods to support their interpretations. While potential-field methods using gravity data are a very powerful tool to define first-order structures along margins such as necking zones or oceanic crust, these methods have limitations in resolving the complex and smaller-scale structure of OCTs. Péron-Pinvidic & Osmundsen (2016) discussed the applicability of such methods to the OCT and showed that these methods are non-unique. In particular, in the hyperextended and exhumed domains where magmatic rocks and serpentinitized mantle occur, these methods are unable to define the nature of the rocks and therefore the geometry and the structure of the OCT (Stanton et al., 2016). In contrast, potential-field methods using magnetic data are more sensitive and can distinguish between magmatic, serpentinites and continental basement rocks in OCTs (Szameitat et al., 2020). Therefore, we will compare our final interpretation with the magnetic map published in Parsons et al. (2017).

Since identifying features on seismic data is by definition an interpretation, we acknowledge that we cannot claim to have the correct answer, but consider our interpretation as one possible solution that is geologically plausible, coherent, and consistent with our current understanding of rifted margins. Thus, although distinguishing between observations and interpretations is not always easy, we consider in this paper the description of well-imaged reflections and related geometries as observations, while in parts of the section where imaging is at low resolution, its description is an interpretation. It is, however, important to emphasize the power of tying and mapping in 3D, which places key constraints on interpretations. To allow the reader to judge the objectivity of the interpretation, we show uninterpreted, partially interpreted and fully interpreted sections. Moreover, this study employs two distinct interpretation steps, the first dealing with the seismic interpretation of reflection geometries that lead to the definition of interfaces and reflection packages (Section 4), and the second being the interpretation of what the geometries may mean (Section 5).

3.3. Terminology

To describe and map the structures defining the rift architecture of the Gabon distal margin, we used the terminology developed by Péron-Pinvidic and Manatschal (2010), Péron-Pinvidic et al. (2013), Sutra et al., (2013) and Tugend et al. (2014; 2015). Fig. 1b summarizes the terms used in this paper.

3.3.1. *Main interfaces*

In order to define the rift domains, we first describe the major interfaces:

- 1) **The Top Salt** is locally a strong and prominent reflection but elsewhere difficult to define. This interface is mostly recording post-depositional events (gravity-driven salt tectonics) and only locally it is related to the structure and evolution of the breakup and the formation of the OCT. Therefore, we combine observations related to salt in the “base salt” sections.
- 2) **The Base Salt** or equivalent weld is a strong negative reflection, although locally it can be weak and difficult to define, especially where deeper.

- 3) **The Top Basement** is visible in some continental areas as a strong event. Where it is difficult to see it is picked at the base of the sedimentary reflections even though we know that the pre-rift successions may comprise some Paleozoic sedimentary basins and that some of the pre-salt sediments may be more seismically transparent. The Top Basement is much clearer in the oceanic domain where it consists of a sub-horizontal, rugose surface changing southward to a more chaotic, irregular surface.
- 4) **The Moho** corresponds to a high-amplitude basal reflection or series of reflections flooring a strongly reflective crust.

3.3.2. Rift Domains and Domain Boundaries

Based on the geometry of the top basement and Moho, the nature of the crust and its relation to the overlying sediments, we define four rift domains and associated domain boundaries:

- 1) **The Hyperextended Domain** is deformed by faults, some of which also affect Moho. Its oceanward termination is the Limit of Hyperextended Continental crust (LHEC, lower section Fig. 2), which corresponds to the oceanward limit of defined continental crust. At this point, the top basement and Moho converge and the continental crust wedges out. The hyperextended crust varies between 12 and 3km thick. Reflectivity in the upper part seems to be affected by faults, while the lower part shows sub-horizontal anastomosing reflections reminiscent of ductile levels.
- 2) **The Exhumation Domain** is defined where the crust is less than 3 km thick and Moho reflections are weak or absent. This domain is at the focal point of reflections corresponding to the top and base of the crust but also of intra-crustal reflections. We cannot determine with the available data if the crust pinches out completely and mantle was fully exhumed or if thin crust was preserved within this domain.
- 3) **The Outer High** is a domain thicker than the oceanic domain and is bounded on its continent side by a trough filled with salt, creating a prominent step in the base salt. It is delimited by the Oceanic

Boundary (OB), which marks the transition to “steady-state” Penrose-type oceanic crust (Gillard et al., 2017), and the Limit of Extrusive magma (LEM).

4) **The Oceanic Domain** is characterized by parallel top basement and Moho reflections and sub-parallel reflections in the upper and lower parts of the crust. The crustal thickness is about 6 km, which is normal for Penrose-type oceanic crust (Dick et al., 2003).

4. Seismic observations

Based on the previous definitions, we describe and interpret three dip and one strike line extracted from the high-resolution depth-migrated 3D survey (Fig. 1a). Each line is 150 to 200 km long. We describe first the major seismic interfaces (base salt, top basement, and Moho). Based on the description of these major interfaces, we define the rift domains. Then we describe intra-basement reflections, including faults, and intra-sediment reflections in order to define tectono-stratigraphic units (post-salt, evaporites, pre-salt sequences) and magmatic additions. Based on this description, we discuss in Section 5 the architecture of the OCT and its tectono-magmatic and sedimentary evolution and then propose a model for its evolution.

4.1. Northern section (Fig. 2)

4.1.1. *Main interfaces*

The **Base Salt** is level at 4.5km depth from the NE end of the line to km 100. The overlying salt is autochthonous and in the extensional domain. Between km 60 and 100, the base-salt reflector is more difficult to follow but clearly affected by faults, making its base strongly irregular. Locally, it can be interpreted to drop down to 8 km depth. The salt structures are complex, showing a transition from the extensional to the contractional domain. Between km 60 and 50, there are indications of two thin salt levels: the base of the upper one ramps up onto a slightly NE-dipping surface that corresponds to an erosional unconformity. From km 45 to 35 there are also two salt levels: a sub-horizontal allochthonous layer between post-rift sediments at 6 km depth, and a strong reflector at 10 km depth

that we interpret as an autochthonous salt body because of the overlying listric fault geometry and associated hanging-wall rollover.

The top Basement over oceanic crust is rough but level at 8 km depth from km 0 to 25. At km 25, it rises to 7 km depth and terminates at km 40. A second strong reflection can be identified at km 45 at about 10 km depth, interpreted as pre-salt sediments overlying basement. From km 45 to 60 a strong reflector with a wavy shape can be identified, between 10 and 12 km depth, that we interpret as top continental basement. From km 60 to 100, the Top Basement is poorly defined but is interpreted to be offset by faults and to drop down to 13 km depth at km 80, where the crust is the thinnest. From there landwards, the Top Basement shallows up to 8 km depth at km 110. From km 100 to 115, the Top Basement corresponds to a strong reflector with a wavy shape similar to the Top Basement at km 45 to 60. While the Top Basement is offset from km 60 to 80 by high-angle faults, between km 80 and 120 it shows long-short-long steps, diagnostic of low-angle extensional detachment faults that break away in the NE and dip to the SW.

The **Moho** is smooth and at 14 km depth from km 0 to 25. From km 25 to 45, it drops down to 15 km depth. At km 30 is a reflection interpreted as a second Moho that dips from km 40 to 50 from 12 to 19 km depth. From km 50 to 70, the Moho can be defined as a concave-up reflection that becomes concave-down from km 70 to 100, with the Moho at 14 km depth at its shallowest point. From km 100 to 125, the Moho is beneath multiple high amplitude, slightly concave reflectors and lies at about 20 km depth.

4.1.2. Rift domains

The **Hyperextended Domain** is between km 85 and 125 and also preserved in a more distal position from km 45 and 75. The top basement is deformed by low- to moderately-dipping faults, some of which also affect the Moho as indicated by the fact that the Top Basement and Moho almost converge, with the crust wedging out from km 110 to 80 and from km 50 to 30 and attaining at both places a thickness of less than 3 km.

The **Exhumation Domain** is only present between km 75 and 85 and is interpreted in the distal domain as a core for the Outer High between km 25 and 45.

The **Outer High** is defined to lie between km 25 and 40. The high, about 9km thick, is floored by a complex, reflective crust with two interpreted Moho reflections. Its top is overlapped by post-rift sediments on both sides.

The **Oceanic Domain** is observed between km 0 and 25.

4.1.3. Intra-basement reflections and faults

Intra-basement reflections in the oceanic crust are subparallel and limited to the upper and lower part of the crust and likely correspond to igneous structures. These reflections can be followed landward, where they form the upper and lower portions of the Outer High before ending. In contrast, the top and base of the continental crust can be followed oceanward and are interpreted to wedge out within the Outer High. As a consequence the LHEC is oceanward of the LEM. In the Hyperextended Domain, reflectivity in the upper crust is greater than in the middle crust, while in the lower part of the crust reflectivity is sub-horizontal and more continuous. This suggests that the crust can be subdivided into a brittle upper part and a more ductile lower part, with the decoupling level about 6 km below the top basement.

Faults occur throughout the section and can be subdivided into four types, shown in the section with four colours, a classification that we will use also in the subsequent sections. The orange faults are related to the Oceanic Crust and include minor normal faults. The black faults are supra-salt and include normal and reverse faults. Most of these comprise proximal extensional faults and distal thrust faults and are therefore post-rift in age and were caused by gravitational salt tectonics. However, there is at least one suprasalt extensional fault that is in the most basinward position, located above the deep salt just landward of the Outer High (km 43).

The most prominent faults interpreted on the section offset the Base Salt from km 100 oceanward, but also occur in the pre-salt section further landward. These faults, shown in violet, die out within the

underlying sediments or at the top basement, but do not propagate upward into the post-salt section. The observation that the normal faults in the pre-salt section affect the Base Salt oceanward but not landward suggests either a younging or a rejuvenation of these faults oceanward. Some violet faults also affect top basement and penetrate the mantle, and so can be considered as coupling faults between crust and mantle. Indeed, two detachment systems are interpreted between km 65 and 125 and between km 30 and 50. These faults break away within the pre-salt section or within the salt, cut through the entire crust and penetrate the lithospheric mantle. A sequence of three extensional detachment faults can be interpreted between km 125 and 95 flooring the pre-salt sequence and/or extensional basement allochthons. At km 80, these faults root where the crust is the thinnest and mantle nearly exhumed. Normal faults in the basement as well as in the overlying pre-salt all converge towards this exhumation point at km 80, resulting in a graben-type architecture at the Base Salt (termed the outer marginal trough by Rowan, 2018, and Curry et al., 2018, and the outer trough by Hudec et al., 2020). It is important to note that activity on these faults span the time from pre-salt into salt deposition. A second detachment system of the same generation can be interpreted between km 30 and 50 and is responsible for the wedging of the crust and the abrupt termination of the pre-salt section, creating a fault offset of about 2 km.

Faults colored violet in Fig. 2 cut through a crust that is already thinned to less than 12km thick. The faults responsible for the necking and thinning of the continental crust and the creation of the accommodation space for the pre-salt sequence are, however, difficult to identify. These faults, shown in blue in Fig. 2, likely sole out in the ductile crust (parallel reflections at the lower half of the crust) and may have been overprinted by the later violet exhumation faults, which may explain why these faults are difficult to identify.

4.1.4. Intra-sediment reflections and tectono-stratigraphic and magmatic units

Based on the intra-sediment reflectivity in combination with the definition of the Top Salt, Base Salt and Top Basement, four tectono-stratigraphic and magmatic units can be defined. We describe these units from top to bottom.

The **post-salt sequence** includes all sediments that stratigraphically overlie the salt and the oceanic crust. While this is easy to define over oceanic crust, the time equivalent sediments over the remainder of the section are affected by salt tectonics and as a consequence can be more difficult to define.

The **salt section**, shown in pink, has two components. The autochthonous salt is thickest in the outer trough, very thin on the high between km 50 and 60 and, between km 45 and 35, at a deep level between the Outer High and the high with the thin salt. Above the high and its capping unconformity is thin salt interpreted as allochthonous, which is thicker and deeper just basinward of the high. Note that the shallow salt does not entirely cover the high.

The **pre-salt sequence** is bounded at its top by the base salt. In the proximal part it has a more reflective, faulted deeper portion overlying a more transparent package at top basement and a less reflective, mostly unfaulted shallow portion. In the central part (km 60 to 100), the pre-salt sequence beneath faulted salt is all faulted and the upper, poorly reflective package is apparently missing, but there is a deep less reflective portion. In the most distal high it is mostly bright, but has a deep, poorly reflective package and a shallow less bright section. It is important to note, however, that the thickness of the pre-salt sequence, which is about 4-6 km, is surprisingly constant across the section, suggesting that it was deposited mainly at a late stage of the thinning, i.e. after necking, but prior to final, syn-salt extension. This is also compatible with the sub-horizontal reflectivity that characterizes the upper part of the pre-salt sequence, which is mostly isopachous. In contrast, the lower sequence is more variable in thickness and contains wedging (growth) sequences that are, however, of a magnitude insufficient to justify the amount of crustal thinning.

Magmatic additions are difficult to define unambiguously in the section outside of the Oceanic Crust. Some magma has been interpreted to occur associated with the Outer High, where it is interpreted to overlie a distal Exhumation Domain and to be overlapped by post-rift sediments. Moreover, the subparallel reflections between km 30 and 40 underlying the outer high may be interpreted as underplated gabbros; however, there is no direct and clear evidence for the occurrence of magmatic additions such as seaward-dipping reflections or magmatic build-ups (volcanos).

4.2. Central section (Fig. 3)

4.2.1. Main interfaces

The base salt is flat and at 6 km depth from km 100 to the NE end of the line. The overlying autochthonous salt is in the extensional domain. Between km 50 and 100 the salt is thicker and the base salt is deformed. Although the base salt is more difficult to follow, it is clearly affected by major faults. At km 70 it is interpreted to drop abruptly from 5 km to 10 km depth. The salt structures in this domain are complex and show a transition from extensional to contractional. From km 70 the base salt ramps up onto a fault-bounded high made of reflective pre-salt sediments. Between km 45 and 20 the base salt is sub-horizontal at 6.5 km depth with a ramp-flat geometry, and the salt pinches out between post-rift sediments. Deeper, but less well imaged, another strong reflector can be identified at about km 45, where a salt body with a deformed top is interpreted at about 10 km depth (constrained by tying in 3D). At this location, we interpret the lower salt as autochthonous and the upper salt as allochthonous.

The top Basement over oceanic crust is rough and level at 8 km depth from km 0 to 20. It then rises in a series of steps to 7 km depth and ends abruptly at km 45. A deeper top basement can be interpreted at km 40 between 10 and 12 km depth. From there to the NE end of the line the top basement is difficult to define. It has an apparently wavy shape and is interpreted to lie between a layer with strong and continuous reflective material reminiscent of sediments and a layer with discontinuous, sub-horizontal reflectivity with a more transparent pattern, which makes it difficult to define precisely the top basement. In our interpretation we put it between 10 and 12 km depth.

The Moho is level and at 20 km from km 100 to the NE end of the line. Between km 50 and 100, the Moho is defined as a concave-down reflection reaching its shallowest point of 12 km depth at km 70. Sub-horizontal reflections below the Moho are interpreted as magmatic additions. From km 50, a reflection interpreted as the Moho rises and terminates at km 35 at about 12 km depth. From km 45 to 20, a reflector interpreted as a second Moho is at 17 km depth that rises to 15 km and remains at this depth to the SW end of the line.

4.2.2. Rift domains

The **Hyperextended Domain** is interpreted between km 45 and 65 and km 80 and 125. The Top Basement is deformed by violet faults, two of which also affect the Moho as indicated by the fact that Top Basement and Moho converge from km 100 to 70 where the crust is thinned to less than 3 km, and also from km 50 to 30. Crustal thickness in the hyperextended crust ranges between 3 and 10 km.

The **Exhumed Domain** is between km 65 and 75 and inferred between km 35 and 45. This domain is located at the focal point of several violet faults, one of them, located at km 70, offsetting base salt by almost 5 km. For this line we cannot decide if the crust pinches out, or if very thin crust was preserved in the exhumed domain.

The **Outer High** is, in contrast to the northern section (Fig. 2), less well defined and masked by the overlying allochthonous salt. We define it between km 25 to 45 by slightly thicker (9 km) crust. Its landward termination is not as clear as further north, but is interpreted at the edge of a narrow trough, and the onlapping on both sides is not well imaged. The Outer High is floored by a complex, reflective crust with no clear reflections, however by tracing reflections from the north into this section, we propose two interpreted Moho reflections.

The **Oceanic Domain** is observed between km 0 and 25 and is consistently 6 km thick.

4.2.3. Intra-basement reflections and faults

Intra-basement reflections in the Oceanic Domain are limited to the upper and lower parts of the crust, as on the northern line. The top and base of the Outer High are dominated by strong sub-horizontal reflections that seem to be transitional into the pre-salt and continental crust. As a consequence, the limit of continental crust is difficult to define and remains highly interpretative. Based on maintaining structural coherency in 3D, we suggest the continental crust wedges out at km 35 within the Outer High. In the Hyperextended Domain reflectivity in the upper crust is more chaotic and affected by faults, while in the lower part reflectivity is sub-horizontal and more continuous. This suggests that the crust can be subdivided, like in the northern section, into a brittle upper part and a

more ductile lower part with a decoupling level at about 5 km below the Top Basement. However, the basement is more transparent than in the northern section and the basement structures are more difficult to determine.

Faults can be divided, similarly to in the northern section, into four types. The orange faults are related to the oceanic crust and include minor normal faults. The faults shown in black are related to gravitational salt tectonics and include normal and thrust faults. These structures sole out in the salt and are of post-rift age.

Normal faults belonging to the violet generation are common in the pre-salt sediments throughout the section but affect the Base Salt only seaward of km 100. The observation that the normal faults in the pre-salt offset Base Salt progressively more towards the ocean may suggest a younging or rejuvenation of these faults basinward. The faults sole out within the underlying sediments or at the top basement. A very prominent fault can be seen at km 70. This fault offsets the Base Salt by more than 4 km and roots into the mantle. This exhumation fault belongs to a lower-angle fault system that breaks away within the salt at km 95 and can be traced from there towards km 70 where it also roots into the mantle. This fault is interpreted to be a classical exhumation fault forming a core-complex like structure at km 70 floored by exhumed mantle. Secondary brittle faults in the basement and the overlying pre-salt sediments can be interpreted on either side soling out into this major exhumation fault. Although much of the activity on this fault system apparently occurred after deposition of the pre-salt section, we cannot rule out the local presence of pre-salt growth strata and thus an earlier initiation. A second fault system of the same generation is interpreted between km 35 and 50 and may be responsible for the wedging of the crust and the abrupt termination of the pre-salt section. However, this fault system is more difficult to interpret and is better documented in the northern section.

Similarly to in the northern section, the violet faults linked to exhumation truncate a crust that is less than 10 km thick. Therefore, the crust had to be thinned already to 10 km before the violet faults initiated. Thus, an older generation of faults likely exists but is enigmatic. These faults, shown by the blue colors, may have soled out in the ductile crust (parallel reflections) and may have been

overprinted by the later generation of exhumation faults, which may explain why these faults are difficult to identify.

4.2.4. Intra-sediment reflections and tectono-stratigraphic and magmatic units

The **post-salt sequence** includes all sediments that stratigraphically overlie salt. While this is undeformed over oceanic crust, the time-equivalent sediments over the remainder of the section are affected by gravitational salt tectonics.

The **salt section** (pink) includes, in contrast to the northern section, a longer allochthonous nappe and the detailed relationships linked to initial salt deposition are less well imaged. At km 45, in between the outer high and the termination of the pre-salt section, a strong reflective layer is interpreted as autochthonous salt deposited over faulted pre-salt sediments.

The **pre-salt sequence** is more complex and reflectivity is less continuous than in the northern section. The overall sequence is between 4 and 7 km thick and was likely deposited during and after thinning of the crust. There are growth geometries in the lower part of the sequence and, to a lesser degree, near the top of the pre-salt section. Thus, the more landward violet faults were active before the onset of salt deposition. However, the more oceanward violet faults (beginning at km 100) offset the base salt and thus were active after deposition of the pre-salt sequence and locally, in particular between km 60 and 80, dismembers the sequence. Again, though, we cannot rule out possible earlier extension in this area. From km 50 to 35 we interpret the pre-salt sequence to be faulted and overlain by magma, an interpretation that is more conceptual and discussed below.

Magmatic additions are difficult to define unambiguously in the section outside the oceanic crust and the Outer High and this is where the comparison with the magnetic anomaly map of Parsons et al. (2017) will be helpful (see discussion below).

4.3. Southern section (Fig. 4)

4.3.1. Main interfaces

The Base Salt is dipping gently oceanward from 4 km to 7 km depth between km 140 and 75. The overlying salt is autochthonous and spans the extensional and contractional domains. From km 75 to 20, the Base Salt is difficult to map but is clearly affected by faults. Locally it can be interpreted to drop down to 10.5 km depth (km 40). Oceanward of km 40, the base salt ramps up to 8 km depth and can be traced seaward between post-rift sediments.

The top Basement is best imaged between km 0 and 20 where it rises from 10 to 8 km depth. Landward, the Top Basement is poorly defined. Between km 20 and 45, it is interpreted to floor the salt, and from km 45 to the NE end of the section the top basement is interpreted to floor a reflective sequence, rising from about 10 to 6 km depth. Unlike in the sections further north, the top continental basement is, except for its seaward termination, not visibly affected by major fault offsets.

The Moho is clearly visible between km 80 and 100 where it dips landward. From km 100 to the NE end of the section, the Moho is deeper than 20 km and not visible in the section. From km 100 to 45, the Moho can be projected from 20 km to 12 km depth. Seaward of km 45, a weak reflection can be postulated terminating at km 20. The oceanic Moho can be followed from km 0 to 35 at about 12-13 km depth.

4.3.2. Rift domains

The **Hyperextended and Necking Domains** can be defined between km 40 and the NE end of the section. Because the Top Basement is poorly defined, its nature is difficult to interpret. Reflections within basement are sparse and show anastomosing geometries, and a subdivision between a more brittle upper and a ductile lower crust cannot be identified in the southern section. One possibility is that there is a different composition and therefore also rheology of the crust.

The **Exhumation Domain** can be defined between km 35 and 50. Exhumed mantle is interpreted to lie at about 10 km depth and to floor the salt sequence. In our interpretation the crust pinches out at km 50.

The **Outer High** occurs between km 5 and 35. An interpreted portion of the Exhumation Domain might partly extend into it between km 20 and 35. The Outer High is overlapped seaward by post-rift sediments and on its continent side it is confined by salt. The outer high is 7 km thick. Its seaward transition is not clear, but it looks as if the crusts on both sides are very thin and neither of classically oceanic (Penrose-type) and/or continental origin.

The **Oceanic Domain** as defined in the sections further north cannot be observed on this section because it presumably is farther to the SW. The crust in the south looks more transitional and is interpreted as a thin oceanic crust with possible oceanic core complexes (i.e. the strong reflection interpreted as an orange fault at km 0 to 5 in the mantle in Fig. 4) even if we cannot exclude the possibility that this reflector is a diffraction or another artefact.

4.3.3. Intra-basement reflections and faults

Intra-basement reflections within the continental crust show sub-horizontal, anastomosing geometries at about 10 to 14 km depth, suggesting that they could represent intra-crustal shear zones. However, well-defined structures are not observable. At the outer high, a band of parallel reflections can be observed wedging out seaward between km 35 and 10.

Faults can, similarly to the previous sections, be subdivided in four types. Again, the orange faults are related to oceanic crust and the black faults are related to salt tectonics and include normal and thrust faults.

Within the pre-salt layers, violet faults as well as a low-angle detachment can be recognized. In proximal areas, many of the faults sole into the detachments but do not offset the base salt. However, the violet faults offset the base salt from km 70 basinwards, suggesting a younging or reactivation of these faults in more distal areas. The detachment within the pre-salt is interpreted to cut down into basement at km 105 and to merge with the Moho, resulting in the pinching out of the continental basement at km 50. The top basement is offset, forming small extensional allochthons above the detachment.

4.3.4. Intra-sediment reflections and tectono-stratigraphic and magmatic units

The **post-salt sequence** includes all sediments that were deposited above autochthonous salt and span the extensional and contractional domains. In the oceanward portion of the profile, the salt is allochthonous and is within post-rift strata.

The **salt sequence**, shown in pink, occurs across the whole section. The most important observation is that salt is thicker between km 25 and 70, which coincides with the location where base salt is affected by faulting and the low-angle detachment merges with the Moho.

The **pre-salt sequence** is well defined from km 80 to 140 where internal complexities indicate the presence of a deeper thin-skinned detachment, whether an older salt or an overpressured shale layer. Seaward of km 80, the reflectivity is less clear, which makes it difficult to subdivide into a lower, more complex syn-kinematic sequence and an upper post-kinematic sequence. It is also important to note that although growth in deepened pre-salt section is interpreted, the overall pre-salt sequence is largely isopachous across the section, ranging from 4 km thick at its proximal and distal ends to 5 km thick in between.

Magmatic additions are difficult to define unambiguously in the section outside the Outer High. At the Outer High, magma has been interpreted to build over exhumed mantle that is sandwiched between underplated gabbros and shallow extrusives.

4.4. NW-SE strike section (Fig. 5)

4.4.1. Main interfaces

The Base Salt can be mapped from km 0 to 20 as a smooth, gently undulating contact. It is apparently missing between km 20 and 35, although the tie with Line 2 suggests there should be a very thin layer of salt. From km 35, it dips down to km 70 and rises to a high at km 95 before forming a wide synformal structure between km 95 and 145. From km 145 to the end of the section the base salt is at about 8 km depth.

The top Basement is difficult to identify in many locations across the section. Between km 0 and 60, it corresponds to a weak but mappable reflection flooring a sequence of continuous reflections interpreted as pre-salt sediments. A normal fault appears to offset the Top Basement by 4 km at km 40. From km 60 to 75, basement is interpreted just beneath the salt. Between km 75 and 100, the Top Basement is reasonably well identified and corresponds to a high overlain by salt. From km 100 to 130, the Top Basement is again poorly defined and is interpreted to correspond locally to the base of salt. From km 130 to the SE end of the section, the Top Basement remains poorly constrained and we interpret it at the interface between continuous reflective layers and a more transparent layer at about 12 km depth, although it could be deeper.

The Moho is well imaged as a basal, high-amplitude reflection between 12 and 17 km depth from km 0 to 60 and km 140 to the NE end of the section. From km 60 to 75 and km 100 to 140, the Moho is poorly defined and interpreted as a sub-horizontal interface at about 10km. Between km 75 and 100, the Moho is weak but can be interpreted as a concave-up structure reaching its deepest point at km 85 at 14 km depth.

4.4.2. Rift domains

The **Hyperextended Domain** extends between km 0 to 60 and km 140 to 175 and consists of 4 to 8 km thick crust. A characteristic of the hyperextended crust is that the Moho flooring this domain is very strong and well imaged. Within the hyperextended crust in the northwestern part of the section reflectors in the upper part seem to be affected by faults, while the lower part shows sub-horizontal continuous reflections, reminiscent of ductile levels. In the southeastern part of the section the basement is more transparent and faults controlling crustal thinning are difficult to define.

The **Exhumed Domain** can be defined between km 65 and 75 and km 105 and 135. For this line we cannot decide if the crust was pinching out, or if an extremely thin continental crust remained preserved in this domain.

An **Outer High** is located between km 75 and 105, interpreted to be formed mainly by magmatic additions up to 6 km thick in this location. The top of the Outer High is affected by normal faults.

An unequivocal clearly defined **Oceanic Domain** is not imaged on this section.

4.4.3. Intra-basement reflections and faults

Intra-basement reflections in the Hyperextended Domain of the northwestern part of the section are interpreted to depict a brittle upper crust and more ductile lower crust. In the southern part of the section, however, the reflectivity is not well developed and/or imaged. In the rest of the section, sparse sub-horizontal reflectivity can be mapped at about 14km depth, while the overlying basement is transparent.

Faults are difficult to define, as expected for a strike line. Nevertheless, a major brittle normal fault can be observed at km 40 offsetting the Top Basement and showing growth structures in the pre-salt section. This observation may indicate that thinning of the basement was oblique to the studied sections or influenced by oblique inherited structures, and it may explain why it is difficult in place to find structures controlling crustal thinning in the dip sections. An alternative is that this structure is a strike slip fault.

4.4.4. Intra-sediment reflections and tectono-stratigraphic and magmatic units

The **post-salt sequence** is in the contractional province along the entire strike line, ***but with shortening from out of the plane***. The salt sequence (pink) is very thin or absent in the high between km 20 and 35, where there is a clear unconformity, and is the thickest over the exhumed mantle domain.

The **pre-salt sequence** displays its most prominent feature at km 40, where a major fault offsets the strata. The basal half of the pre-salt section thickens into the fault, indicating that it formed during deposition of the early pre-salt sequence. Elsewhere the pre-salt is largely isopachous, but any impact by the extensional event associated with the violet faults is difficult to determine on this strike profile.

Magmatic additions are difficult to define unambiguously in the section. We interpret magmatic additions to constitute the block between km 75 and 100. The reflectivity and the nature of top and base of the block are distinctly different from those over hyperextended crust and, when combine with tying in 3D, justify the interpretation that this block is made of magmatic additions.

5. OCT Architecture

The interpretation of the 3D seismic survey, illustrated in the dip and strike lines of Figs. 2, 3, 4 and 5, allows us to describe the crustal architecture of the OCT of the southern Gabon margin shown in the map in Figs. 6a and 6b. Our results show a complex architecture with proximal to distal and along-strike changes in the nature of continental basement, the volume of magma and the deformation style, which have important implications on the tectono-magmatic and stratigraphic evolution as well as for the depositional history during breakup.

5.1. Crustal architecture

The architecture of an OCT reflects the interaction between two first-order processes: 1) extension of existing continental lithosphere (rifting), and 2) accretion of new oceanic lithosphere (drifting/seafloor spreading). In the study area, we can map in detail the results of these two processes that result in hyperextended crust (rifting) and oceanic crust (drifting/seafloor spreading). In between these two different types of crusts one can find exhumed and hybrid/magmatic crusts. In the previous sections we described the characteristics of each of these domains in dip and strike directions. A key, pattern, which is shown nicely on the strike line (Fig. 5) is that the various domains show some first-order differences: the hyperextended domain shows a well-imaged deep Moho and shallow base salt; the exhumed mantle domain is characterized by a lack of clear Moho reflections and a deep base salt, the outer high in contrast shows complex reflectivity in the basement and the base salt steps up basinward; while oceanic crust has a well-defined base and top basement and overlying salt is, where present allochthonous. Below we describe the different units and integrate them in map view (Fig. 6b).

The **hyperextended crust** is reasonably well imaged and is characterized by its thickness (ranging from 10 to 3 km), its shape (showing wedging architectures) and its cover (a thick syn-rift pre-salt

sequence). The architecture and related structures in the hyperextended crust appear different in the northern (seismic profiles 1 & 2, Figs. 2 & 3) and southern (seismic profile 3, Fig. 4) sections. In the north the crust is subdivided between a reflective lower part with sub-horizontal reflections and a more complex upper part. The upper part is affected by normal faults that create a fault-bounded top basement and sole out about 5 to 6 km deeper. In the south, the hyperextended basement does not show the classical subdivision between ductile lower and brittle upper parts. The upper part is not controlled by mappable faults, suggesting that thinning of the crust may have occurred by more ductile pure-shear extension. This difference may reflect a change in the nature of the crust or the intensity of the deformation, which may in turn be controlled by compositional inheritance (a stronger, quartzo-feldspathic crust in the north and more mica-rich/meta-sedimentary units controlling the bulk rheology of the crust in the south (Manatschal et al., 2015)) or by a more important input of pre-salt sediments toward the south. The change in the nature of the crust is well documented in the strike line (seismic section 4, Fig. 5).

Exhumed crust/mantle occurs all along the sampled margin and is in between unequivocal continental and hybrid magmatic and oceanic crusts in the south (Fig. 4), or preserved in between pieces of hyperextended crust in the north (Fig. 2). Note also that this domain correlates with low magnetic values that contrast with the much higher values on the adjacent continental crust and outer high (Figs 6c and 6d). This type of crust is characterized by its crustal thickness (< 3 km), the lack of well-defined Moho reflections, a top basement and base salt that are deeper than in the surrounding hyperextended and oceanic domains. Exhumation may locally be of lower continental crust or subcontinental mantle (or both), which can be overlain by rafts/allochthons of continental origin (continental crust or pre-salt sediments), magmatic additions and salt. The exhumed material is linked with a failed rift axis that tips out northward resulting in a horst-graben type structure with exhumed crust/mantle separating blocks of hyperextended crust and a thick pre-salt sedimentary sequence (see section of Fig. 2 and map in Fig. 6b). In the south and seaward of the northern propagator, magmatic additions are emplaced over exhumed mantle and form the western boundary of this domain. The observation that exhumed domains are linked to propagators and can be found on both sides of

continental blocks (e.g. continental block in Fig. 2) suggests that exhumation occurred along segmented systems within a previously hyperextended domain. Relay ramps, truncated during the subsequent breakup, can explain the complex location of exhumed mantle shown in the map in Fig. 6b. This is similar to what has been reported from the Iberia margin (see Fig. 9 in Péron-Pinvidic et al., 2007). Similar to Iberia, the exhumation occurred beneath exhumation faults, but there are two major differences in the southern Gabon example: 1) exhumation occurred in a significant depositional environment (thick pre- and syn-salt sediments) when detachment faulting occurred, and 2) magma was apparently emplaced shortly after or during mantle exhumation (Epin et al., 2019). As a consequence, the exhumed mantle domain in the northern failed rift axis preserved the extensional structures on both sides, while in the south the oceanward termination of the exhumed domain is formed by magmatic additions that interfere with the previously exhumed domain.

The exhumed domain is rimmed oceanwards by a structure that we refer to as the **outer high** that separates the OCT from normal, Penrose-type oceanic crust, defined by a 6-7 km thick crust with parallel top and base crust. The outer high is characterized by thicker crust and a shallower top basement. Its top and base can be correlated towards oceanic crust and are most likely magmatic in origin. This is further supported by the correlation with a positive magnetic anomaly that correlates with the location of the outer high (Figs. 6c and 6d). In contrast, on its landward side residual crust (hyperextended or exhumed) can be interpreted to pinch out within the outer high (see section Fig. 2). This observation is reminiscent to that described by Gillard et al., (2017) , where exhumed mantle and/or thinned crust is sandwiched between magmatic intrusive and extrusive bodies, forming a hybrid crust also referred to as “crocodile-type” structure. Thus, we interpret the outer high as the result of the first important magmatic additions that initiate and form during final breakup of the lithosphere. Some authors also used terms such as proto-oceanic crust (Gillard et al., 2015, 2019), or embryonic oceanic crust (Manatschal and Müntener 2009) to describe this outer high. In the example of Gabon, it can be seen that such magmatic additions can build individual highs several tens of km long, up to 20 km wide and up to 2 km high (above the level of normal oceanic crust) that are bounded by areas of exhumed mantle (Fig. 6b) and overlapped by post-rift sediments.

In summary, the crustal structure of the OCT in southern Gabon consists of exhumed and hybrid crusts separating unequivocal continental and oceanic crusts by tens of kilometers. The OCT can be formed by extensional windows floored by exhumed crust and/or mantle and highs that comprise fault bounded exhumed material, faulted upper crustal/pre-salt sediments, magmatic additions, or some combination.

5.2. Deformation style

The formation of rifted margins is the result of polyphased extension including different modes of deformation. In this study we only focus on the most distal part of the southern Gabon margin and more precisely on the OCT. Thus, in our sections we can only see the structures that shaped the most distal parts of the margin during final rifting. In this part of the margin we can distinguish four events. In order to simplify their description in the seismic interpretations, we refer to the orange, black, violet and blue events.

The **orange event** includes normal faults affecting the outer high and oceanic crust. Since their formation occurred during a clear syn- to post-oceanisation setting, their importance for the formation of the OCT are minor and we do not further detail this event and the related structures.

The **black event** records mostly gravity-driven salt tectonics. The related structures are extensional and contractional and occur only post-breakup, and they are not considered further here. However, there is an anomalous listric fault on the northern line above the most distal, down-dropped autochthonous salt (km 43, Fig. 2). This fault is extensional and soles into salt like other black faults. Thus, it may be gravity-driven like the others, but because it is basinward of the contractional domain it would have to be part of a separate gravitational system and linked to contraction that is now on the conjugate margin. A more likely interpretation is that it represents ongoing crustal extension, but decoupled by the salt. This is supported by the observation that extension on this fault ceased at the exact stratigraphic level of the top of magmatic crust, in other words when rifting switched completely to the creation of new oceanic lithosphere.

The **violet event** is the main structural event observed in the seismic sections and it is intimately linked to the formation of the OCT. The most characteristic structures linked to this event are steep extensional faults that are well imaged in the pre-salt section and belong to detachment systems that crosscut a thinned residual crust, with exhumed lower crust and mantle in their footwalls. These structures are well imaged in the northern and central sections (Figs. 2 and 3).

It is important to note that the observed space-time relationships between faulting and sediment/salt deposition changes from proximal to distal. In the more landward area, the violet faults were active in the early pre-salt, but had minimal impact on the later pre-salt sequence and did not affect the base salt. In contrast, in the more basinward OCT, faults offset the base salt and may also have been active during the late pre-salt.

The **blue event**, which pre-dates the violet extension, is poorly defined and difficult to interpret on the seismic data. This is well shown by violet detachment faults truncating a < 10 km thick residual crust (Figs. 2 and 3). This leads to the question of what processes can explain crustal thinning to 10 km and even less. In the sections, there are few observations that can provide constraints on the thinning processes. In the northern sections (Figs. 2 and 3) the reflectivity in the crust shows evidence for ductile deformation in the lower crust and hints for brittle deformation in the upper crust prior to the onset of the violet faults. In the southern section (Fig. 4) it appears as if the whole crust was deforming by pure-shear extension. This suggests a change of the mode of crustal thinning from the north, where crustal thinning may be explained by strain partitioning during crustal necking between brittle and ductile layers (e.g. Fig. 14 in Mohn et al., 2012), to a more distributed ductile pure-shear thinning in the south (Clerc et al., 2018; Sapin et al., accepted). The limit between these two crustal domains that show different deformation styles, interpreted to be linked to different crustal rheologies and compositions, correlates well with the magnetic map of Parsons et al. (2017) showing a major change of the magnetic signal between the north (sections 1 and 2) and the south (section 3) (see Figs. 6c and 6d).

5.3. Stratigraphic architecture

The stratigraphic architecture and evolution of OCTs are poorly defined due either to a lack of drill hole data and/or good imaging (masking by salt and/or magma), or to sediment starvation such as along the Iberia-Newfoundland margins where the syn-rift sequence is poorly resolved in seismic interpretations because it is too thin. In the southern Gabon margin, there are no drill holes that penetrate the OCT in the distal margin. There are, however, drill holes in more proximal areas that provide information about the salt and pre-salt sections (e.g. Dupré et al., 2007; Total internal communication). Moreover, seismic imaging is generally good and in the northern section much of the OCT is not masked by thick salt. In addition, sedimentation rates were very high, which makes sedimentary units well resolved.

In this study, we focus on the first order stratigraphic architecture of the OCT and subdivide it into three main units: 1) the pre-salt unit, 2) the salt unit, and 3) the post-salt unit. Both the pre-salt and salt units are syn-rift sensu Ribes et al. (2019), i.e. these units have been deposited during rifting and are considered to have formed between the Neocomian and Latest Aptian. An early rift phase (pre-Middle Barremian) is well exposed in the proximal margin and occurred in continental depositional environments (Guiraud & Maurin, 1991). Remnants of this early event are not clearly observed in the OCT but cannot be excluded to floor the pre-salt sequence locally. The second rift event resulted in the migration and focusing of extension towards the locus of future breakup and is associated with a thick sedimentary sequence, also referred here to as the pre-salt unit that is overlain by the salt and post-salt units.

The pre-salt unit is dated from the Middle Barremian to Late Aptian (~127-113Ma) and is associated with thick fluvial to lacustrine and minor shallow-marine environments (Dentale Fm, Fig. 1, Dupré et al., 2007). In the proximal portions of our sections we observe growth structures and lateral thickness variations, more in the lower part of the pre-salt syn-tectonic packages but also locally in the upper part. The base of the sequence is fault bounded in the northern area (Figs. 2 and 3). In the southern section (Fig. 4) many of the faults sole into an obvious thin-skinned detachment (either salt or shale) and display hanging-wall growth geometries throughout the middle and upper pre-salt sequence. Deeper faults are apparent but difficult to interpret. The thin-skinned extensional system

may represent gravitational failure, but we see no matching contraction in more distal positions. Instead, we consider it more likely that this is a form of decoupled thick-skinned extension, with the supra-detachment faults balancing ongoing crustal rifting in more distal locations during pre-salt times.

Farther seaward, the salt thickens in the hanging walls of violet faults, forming the outer trough. Offset of the base salt can be explained by some combination of three possible relationships (see Rowan and Jarvie, 2020): 1) the salt is locally syn-tectonic and represents growth strata; 2) the salt is locally post-tectonic and filled relict topography during deposition; or 3) the salt is locally pre-tectonic and flowed into the space subsequently created by extension. The second and third options require either a pause in deposition prior to salt deposition or a pause in extension, respectively; thus we favor the interpretation of the salt as growth strata.

While in the northern sections the fault-bounded salt overlies a thick pre-salt section, in the south, salt is interpreted to directly overlie exhumed mantle. Thus, the salt architecture and possibly even the depositional conditions may change along-strike.

The post-salt unit is almost entirely post-rift and deformed by gravity-driven salt tectonics. However, as described above, the most distal suprasalt fault on the northern line (Fig. 2) probably formed during thick-skinned extension. The implications, in this part of the margin at least, are that the onset of spreading occurred after the salt was buried and that the oldest suprasalt strata are syn-rift, not post-rift. We speculate that the faulted section that abuts the landward edge of the Outer High might be an expanded earliest Albian sequence.

6. Discussion

In the following section, we discuss our results for the architecture of the OCT offshore southern Gabon by proposing a tectonic model for the breakup history of this margin. The aim is to explore the implications of this model for the processes controlling breakup and evaporite deposition in a salt-rich margin at the rift to drift transition.

6.1. Tectonic model for the evolution of the OCT

The observations described above concerning the crustal architecture, the styles/events of deformation and the tectono-stratigraphic sequences can be summarized in a tectonic model shown in Figure 7. In order to explain the different architectures and the evolution of the southern and northern parts of the OCT of the southern Gabon margin, we show and discuss the evolution of the two parts in parallel in Figure 7.

6.1.1. From crustal thinning to hyperextension

Our observations provide little constraints about how and when crustal thinning occurred. The timing of necking is uncertain, but may have been late Barremian and may have initiated with the termination of rifting at the proximal margin (e.g. transition from rift phase 1 to rift phase 2; Guiraud & Maurin, 1991). Whatever the timing, it appears that the thinning process in the north and the south were slightly different, probably due to compositional variations in the crust as nicely shown in the magnetic map in Fig. 6c and d. This may explain a more intense ductile and distributed deformation in the south than in the north. Crustal thinning was accompanied by the creation and at least partial filling of accommodation space.

The observation that the lower parts of the pre-salt locally show growth structures suggests that this unit formed during the onset of the violet faults. This likely marked the transition to hyperextension once the crust was less than 10 km thick and completely embrittled. The relative lack of extension in the upper presalt, coupled with the offset of the base salt in more distal positions, has three possible explanations. First, deformation during late pre-salt times may have migrated westwards and the coeval syn-tectonic sequences should be preserved at the present-day conjugate margin (eastern Brazilian margin). Second, rifting ceased and the late pre-salt was deposited during a pause of extension and an early thermal equilibration. Third, and our preferred solution, is that rifting shifted from the area of unfaulted base salt to the position of future breakup during final pre-salt and earliest salt deposition (Fig. 7a). We postulate that fault-bounded lows were filled by expanded latest pre-salt strata now preserved beneath the down-dropped salt in the outer trough (Fig. 8). Moreover, these sediments may have been interbedded with salt layers during the transition to evaporite deposition,

with subsequent mobilisation during ongoing rifting and subsequent deformation resulting in a bright, chaotic seismic character with no clear base salt (e.g., Figs. 2-4 and similar images in Rowan, 2018).

6.1.2. From hyperextension to exhumation

The salt depocentres are clearly fault controlled and the faults offsetting the base salt are kinematically linked to detachment faults and mantle exhumation (Figs. 7a, b). We assume that deformation in the sedimentary section was distributed and occurred over a wide area before it localized over the areas where extensional detachment faults exhumed lower crust and mantle. This phase is also called the coupling phase (Sapin et al., accepted). Salt deposition continued during exhumation of the mantle (Fig. 7b), with the exhumation occurring beneath a thick pre-salt sequence, up to 4 to 6 km thick, in the north. In the south, however, salt lies directly over exhumed mantle and the question discussed below is whether this observation suggests deposition of salt over exhumed mantle or a more complex interaction between salt deposition, salt flow and ongoing exhumation. While models based on potential-field modelling show a continuous deep Moho beneath the outer trough (Fernandez et al., 2020), the high-resolution 3D seismic data clearly show that the Moho gets very shallow beneath the outer trough, which is compatible with an exhumation model (see also Rowan, 2018). Indeed, potential-field methods using gravity data can't necessarily distinguish between exhumed serpentinized mantle and magmatic rocks since the densities of these rocks can be similar.

6.1.3. From exhumation to seafloor spreading

Seafloor spreading and formation of a Penrose oceanic crust was preceded by magmatic additions but also by an apparent rifting that outlasted salt deposition, at least in the northern part of the South Atlantic salt basin, as shown by distal suprasalt normal faults that are interpreted to represent decoupled thick-skinned extension (Fig. 2). This relatively late formation of oceanic crust may be related to the northward younging of rifting and spreading in the South Atlantic. The thick-skinned extension appears to have mostly predated magmatic activity.

Localized, discontinuous and punctual magmatic additions, similar to what can be observed in the present northern Red Sea (Bonatti, 1985; Ligi et al., 2018) occurred after exhumation and salt

deposition Fig. 7c). The magma was emplaced as intrusive and extrusive bodies over previously exhumed or pre-deformed crust (Epin et al., 2019). No evidence of flows can be found, suggesting that magma emplacement was below sea level. From all our observations we cannot see evidence that magma was forming simultaneous to salt deposition as proposed by Fernandez et al. (2020), but it appears as if it post-dated salt deposition. Moreover, magma was not necessarily following inherited structures but cut across and eventually separated a previously complex extensional template, leaving behind a structurally complex OCT (Fig. 7d).

The final breakup may have occurred in two different ways. Either magmatic additions formed first in the south, over exhumed mantle (as depicted in Fig. 7b), and propagated northwards by intruding into an active, pre-deformed system and thereby forcing the breakup. Alternatively, magma may have formed along the whole segment simultaneously and may have overprinted and separated a complex rift template deformed by segmented exhumation axes. Breakup occurred in a system with exhumation faults and some of them aborted prior to oceanic accretion resulting in a complex along-strike architecture of the OCT. In the studied example, final magmatic breakup truncated an aborted axis at an angle of $\sim 20^\circ$ (Figs. 6 and 7). This observation can be explained by either a change in kinematics or, more likely, breakup connecting segmented hyperextended systems across relay ramps. Alternatively this could also be explained, as modelled by Brune et al. (2014, 2017), as the result of rift migration toward the final axis.

6.2. *Timing and depth of salt deposition*

The timing and depth of salt deposition and the controlling tectonic processes are topics of lively debate in the international community working on deep-water salt basins (e.g. Gulf of Mexico, Mediterranean, South Atlantic; for a review see Rowan, 2018). Many recent papers addressed the relative timing of salt deposition and the related depositional environments for the Central segment of the South Atlantic. Karner and Gambôa (2007) and Reston (2010) discussed the conditions and timing of salt deposition and proposed either a possible delayed thermal subsidence or basin isolation and sea-level drop to explain salt deposition. Norton et al. (2016) suggested that the present-day salt limits do not coincide with the limits of oceanic crust and concluded that salt was deposited as seafloor

spreading started and that salt flowed over the ridge axis sealing off the extrusive component of oceanic crust and resulting in the formation of intrusive oceanic crust. Pindell et al. (2014) introduced the idea of an outer marginal collapse at the rift-to-drift transition, an idea invoking rapid tectonic subsidence linked to landward dipping faults during final rifting. According to these authors this process could create more than 3 km of subsidence over less than 3 Myr and could account for the stratigraphic and structural relationships interpreted at many distal margins. Using this model, salt would have formed at sea level, but in a rapidly subsiding and collapsing asymmetric basin just prior to breakup. Cowie et al. (2016) tried to constrain the paleo-bathymetry of the base salt along the northern Angolan rifted margin using flexural back-stripping and reverse post-breakup thermal-subsidence modelling. The preferred model proposed by the authors was that the proximal salt was deposited between 0.2 and 0.6 km beneath global sea level and subsided by post-rift thermal subsidence, while the distal salt formed during late syn-rift, when the underlying crust was actively thinning, resulting in additional tectonic subsidence. Rowan (2018) suggested that salt was deposited during the final stages of rifting with depositional relief of the top salt, ranging from near sea level at the basin margin to as much as 2-3 km deep in the basin centres. Debure et al. (2019) pointed out the inconsistency between the wet and warm climate conditions reconstructed for the period of salt deposition and the deposition of mega-evaporitic sequences generally assumed to occur in a more arid climate. These authors therefore suggested a link between salt deposition and mantle exhumation that can absorb water in mantle rocks during serpentinization, and called this kind of evaporite a “dehydratite” deposit. Thus, from this short review of recently published papers it is clear that the relative timing of salt deposition relative to breakup, mantle exhumation and rifting is not well established, and that neither the depth of salt deposition relative to sea level nor the processes related to salt deposition are well constrained. All these subjects remain debated in the scientific community.

In this study we had access to one of the best seismic datasets of the southern Gabon margin and probably of the whole Central segment of the South Atlantic, with the advantage that the study was located at the only place where salt is not hugely gravitationally overflowing the OCT and where

seismic imaging can determine the geometrical relationships of salt deposition and the relative timing of breakup.

The relative timing of salt deposition in the OCT of the southern Gabon margin is constrained in our study by the observation that detachment faults break away in the pre-salt sequence and that some of these faults also offset the base salt and are linked to the creation of accommodation space in the salt (Figs. 2 to 5). This is a direct proof that salt was deposited during mantle exhumation. Moreover, from all our observations we cannot see evidence that magma was forming simultaneous to salt deposition as proposed by Fernandez et al. (2020) or suggested by Norton et al. (2016), which might, however, be the case further to the south. At the southern Gabon margin magma emplacement clearly post-dated salt deposition. We also have evidence that, at least in the north, rifting continued even after the end of salt deposition (Fig. 2). Thus, based on our observations, salt deposition occurred simultaneously with mantle exhumation, during final rifting and before lithospheric breakup (Fig. 7).

The depth of salt deposition at the proximal margin is well constrained and salt has been shown to form in shallow water near sea level. It may also have been deposited in shallow water in the distal parts of the margin, near the centre of the salt basin prior to break up. There was clearly relief on the base salt due to ongoing rifting, but the top could have remained near sea level. The observation that the pre-salt sequence consists of thick fluvial/lacustrine to shallow marine sequences may be interpreted to show that sedimentation and subsidence rates compensated each other over a very large scale while thinning was propagating seaward. Moreover, the predominant sub-aerial conditions might suggest deposition near or even above sea level, compatible with an apparent retardation of subsidence (Dupré et al., 2007). Also, the occurrence of an erosional surface on top of a high block in the OCT (Fig. 2) could indicate that this block was emergent and above sea level during mantle exhumation.

However, these observations do not necessitate evaporite deposition near sea level. First, it is critical to distinguish between water/brine depth and depth relative to sea level – it is possible to have shallow water or even nonmarine conditions well below sea level if the basin is isolated from the world ocean. The basin was clearly isolated by the time of evaporite deposition, but even the presalt strata farther

south in the same basin were deposited in highly saline, highly alkaline environments (Saller et al., 2016). Second, in our interpretation, the erosion of the high occurred after salt deposition, so that its timing relative to exhumation is unknown. Moreover, erosion can happen in even deep-marine environments (e.g., Weaver & Thomson, 1993; Howe et al., 2001).

The key question is at what depth salt formed in the distal domain over the area where mantle was exhuming. Although salt deposition occurred simultaneously with mantle exhumation, it is important to note that the mantle started to exhume not at the seafloor in the northern area, but below a sequence of 4 to 6 km of pre-salt sediments. Thus, a depth near sea level does not necessarily suggest unusual conditions and/or require thermal support due to anomalous asthenospheric processes or dynamic topography. In the southern section, however, salt is interpreted to directly overlie exhumed mantle and thus may have been deposited at a similar depth. Alternatively, it may have been deposited at shallower levels and subsequently juxtaposed against the mantle after its formation by ongoing extension and exhumation and/or by allochthonous flow from more proximal positions.

Thus, a possible interpretation is that salt formed in a late stage of extension, during mantle exhumation and local tectonic subsidence and regional thermal subsidence due to thermal recovery of the thinning phase. Evaporite deposition may have been maintained at shallow levels as it kept pace with tectonic subsidence, but with relief of the base salt ranging from lows caused by coeval extension in the outer trough to an almost emergent high (Fig. 9a). This interpretation requires locally large thicknesses of salt, with very rapid subsidence dropping the salt to deeper levels around the time of the onset of spreading.

However, if salt deposition was not able to keep up with subsidence one would expect that it formed at greater depths below sea level. There is evidence to support this. First, the oldest supra-salt strata vary from proximal platform carbonates to pelagic facies going oceanwards (Brink, 1974; Teisserenc & Villemin, 1990), implying varying bathymetry of the top salt immediately after its deposition. Second, the relative levels of salt and oceanic crust provide critical information by using the concept of “regional” (Hossack, 1995), i.e., the level of a horizon where it has not subsequently been deformed

other than by regional uplift or subsidence. Very importantly, there is no geometric record of any abrupt difference in thermal or loading subsidence between the outermost salt and the oceanic crust, indicating that there was only gradually increasing subsidence from proximal to distal since evaporite deposition and the onset of spreading; this is especially clear around km 40 on the northern line (Fig. 2). Constructing the regionals for the top oceanic crust and the base salt shows a difference between the two of approximately 1.3 km in the north (Fig. 10) and close to zero in the south. Assuming the first oceanic crust formed at 2.7 km (Cowie et al., 2016) and allowing for compaction of the pre-salt strata but not the oceanic crust, the base of salt would have ranged from roughly 1 km to over 2 km depth from north to south. The salt was originally thin on the basement highs, as shown by the geometries on the eroded block in Fig. 2, so the depositional level would have been only slightly shallower. Thus, the evaporites would have been deposited in an underfilled basin with relief on the top salt (Fig. 9b). Coeval rifting in the outer trough would have dropped the base salt, with the generated accommodation space filled with some combination of further salt deposition and flow of salt from surrounding highs (Fig. 9b).

Some might consider the interpretation of a deep isolated basin prior to salt deposition, with evaporites forming 1-2 km beneath global sea level, as unrealistic. One reason is that we do not see evidence for incised deep canyons in the pre-salt section. But that would be expected for an abrupt Mediterranean-style drawdown of a preexisting water-filled basin (e.g., Ryan, 2009). The combination of gradual subsidence during pre-salt and salt deposition, a consequent gentle regional depositional surface, and non-marine to lacustrine settings, as interpreted here, would not require the incision of canyons.

We do not consider, as suggested by Debure et al. (2019), that serpentization was a main trigger for salt deposition as in the north the mantle was never exhumed and remained below 4 to 6 km of pre-salt sediments and may likely be very little serpentized. Nor can an origin related to mantle exhumation explain the widespread deposition of salt in more proximal positions or the already highly saline and alkaline conditions in the upper pre-salt farther south in the same basin (Saller et al., 2016). We can also exclude, based on the observations presented in this paper, that salt formed during magmatic activity and/or during breakup as suggested by Norton et al. (2016) and Fernandez et al. (2020). We

consider that the most likely interpretation is, as already proposed by Rowan (2018), that salt formed at different depths and we concur with Cowie et al. (2016) that salt deposition occurred during exhumation and has an important impact in the estimation of paleo-water depth at distal rifted margins.

7. Conclusions

The access to high-resolution seismic data from the southern Gabon distal margin enabled us to propose an architecture of the OCT in the area, to propose a tectonic model for the breakup history at this salt-rich margin and to explore the implications of this model for salt deposition during final rifting in the Central segment of the South Atlantic. The main conclusions of this study are:

- The OCT is formed by a series of rift axes floored by exhumed crust and/or mantle that initiated during deposition of a thick pre-salt sequence. Some of these axes may have failed and been preserved on one side of the conjugate margins.
- The relative timing of salt deposition is constrained by the observation that detachment faults exhuming mantle break-away in the pre-salt sequence and that some of these faults also offset the base salt and are linked to the creation of accommodation space in the salt during mantle exhumation.
- From all our observations we cannot see any evidence that magma was forming simultaneously with salt deposition.
- Our observations suggest that salt may have formed at different depths in the distal parts, near 1 km below sea level over a thick pre-salt sequence in the north and closer to 2 km deep in the more extended southern part.
- The conclusion that salt deposition occurred at depth during exhumation and was syn-kinematic has an important impact in the estimation of paleowater depth at distal rifted margins.

Acknowledgements

We are grateful to CGG Services SAS for getting access to the publication of four high quality seismic sections from their 3D Gabon survey within the frame of their participation in the M5 consortium. This work was funded by Total through a postdoc grant to Marie-Eva Epin. We would like to thank Total S.A., Jean-Noel Ferry (manager of RTPM R&D project) and Frank Despinois for funding and supporting the postdoctoral project and in particular the Congo-Gabon exploration team and Thomas Maurin for our discussions on the 3D volume and the regional context. We also would like to thank Oscar Fernandez for his very constructive review.

Figure captions

Fig. 1: a) General map of Gabon showing the seismic dataset of CGG (black polygon) and the approximate position of the seismic sections presented in Figs. 1b and 2-5, the ocean boundary (red stars after Karner et al., 1997; and red dots after Lentini et al., 2010), distal salt limit (pink dashed line after Lavier et al., 2001), and gravity anomaly (mGal) from Sandwell et al. (2014). b) Large-scale interpretation of the northern Angola margin (from Péron-Pinvidic et al., 2017) based on the interpretation of an ION regional seismic section. c) Stratigraphic section from the G2 well (Dupré et al., 2007) and Total internal reports based on tens of pre-salt wells.

Fig. 2: Seismic profile 1 (see Fig. 1a for location) through the northern part of the study area. Seismic section at top, line drawing with major interfaces in the middle (dotted where uncertain), and interpretation below. See text for description.

Fig. 3: Seismic profile 2 (see Fig. 1a for location) through the central part of the study area. Seismic section at top, line drawing with major interfaces in the middle, and interpretation below. See text for description.

Fig. 4: Seismic profile 3 (see Fig. 1a for location) through the southern part of the study area. Seismic section at top, line drawing with major interfaces in the middle, and interpretation below. See text for description.

Fig. 5: Strike seismic profile 4 (see Fig. 1a for location) through the western part of the study area. Seismic section at top, line drawing with major interfaces in the middle, and interpretation below. See text for description.

Fig. 6: Simplified interpretative map of the OCT in the southern Gabon margin showing the lateral variation of the distal domain: a) at the scale of the south Gabon margin, b) a close-up highlighting the major violet fault event and the trend of the aborted rift axis compared to the ocean boundary (red line), c) magnetic map showing a differential reduction to pole (dRTP) transformation on the marine magnetic data taken from Parsons et al. (2017), and d) overlap of the geological interpretation with the dRTP magnetic map showing a good correlation between the mapped rift domains and the magnetic data.

Fig. 7: Schematic evolution of the northern (left) and southern (right) parts of the study area. a) ~121Ma (early Aptian): onset of hyperextension and final deposition of the thick pre-salt sequence along with proposed earliest salt deposition (see Fig. 8). b) ~113Ma (late Aptian): hyperextension and exhumation of the mantle, deposition of the main evaporitic sequence. c) ~112Ma (Aptian/Albian): formation of the Outer High domain. d) Present-day situation. a') to c') are corresponding map-view representations, d') shows the situation during early breakup. The depositional surface in a) and b) is shown at sea level but was probably deeper (see text).

Fig. 8: Hypothetical evolution during upper pre-salt and salt deposition. a) End of lower and middle pre-salt deposition. b) Upper pre-salt deposition (Vembo-Gamba), with thickening in developing outer trough. c) Initial evaporite deposition in outer trough, with no deposition and/or minor erosion on relative highs. d) Situation after multiple cycles of evaporite and non-evaporite layers in outer trough, followed by first salt deposition on highs. e) Present-day situation, with interbedded non-evaporite layers in base of outer trough disrupted by salt mobilisation.

Fig. 9: Schematic 3D models of end-member interpretations for salt deposition. a) Salt filled all the accommodation space and compensated tectonic and thermal/loading subsidence, with salt deposited everywhere at shallow depths below sea level. b) Salt did not keep pace with subsidence and was deposited with primary relief, from shallow-marine conditions in proximal areas to 1-2 km below sea level in distal domains. In the south, exhumation was able to strip away the thick pre-salt section, and down-dropping of the base salt may have led to gravitational flow into the areas of exhumed mantle.

Fig. 10: Illustration of “regional” datums for the top oceanic crust and base salt on the northern profile, which differ in the OTC by 1.3 km. The base salt is below regional in the outer trough and adjacent to the Outer High due to extension, and above regional in the footwalls of the major exhumation faults due to isostatic uplift.

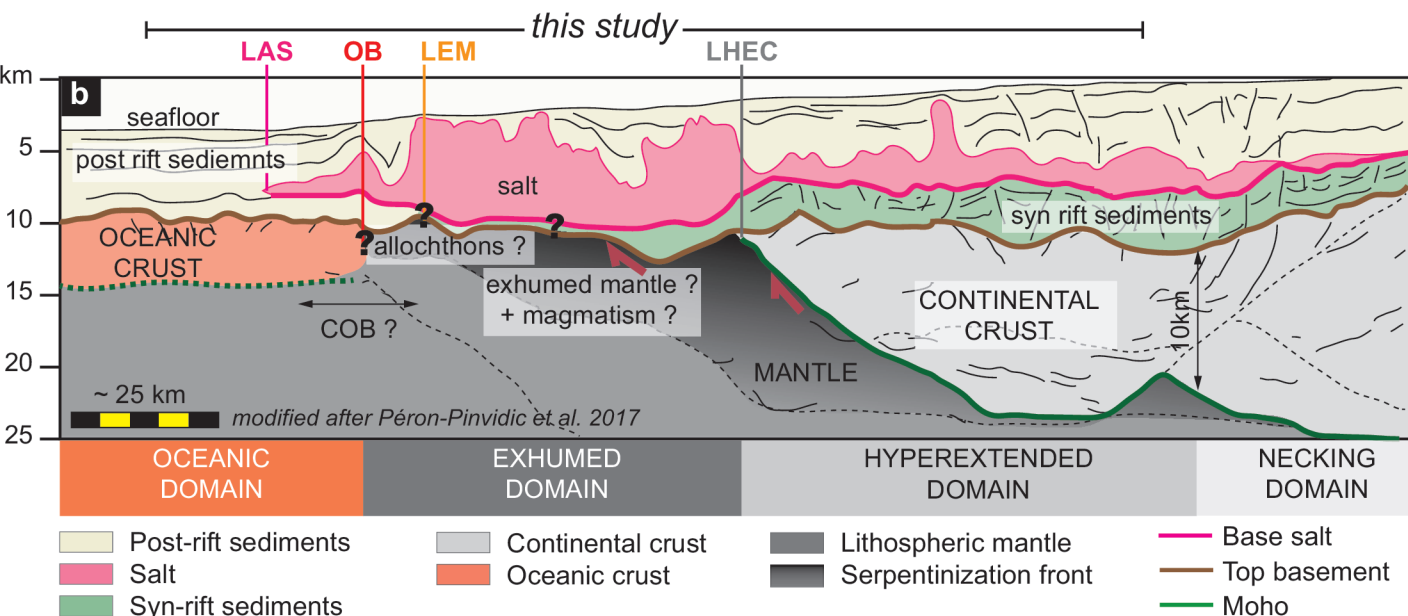
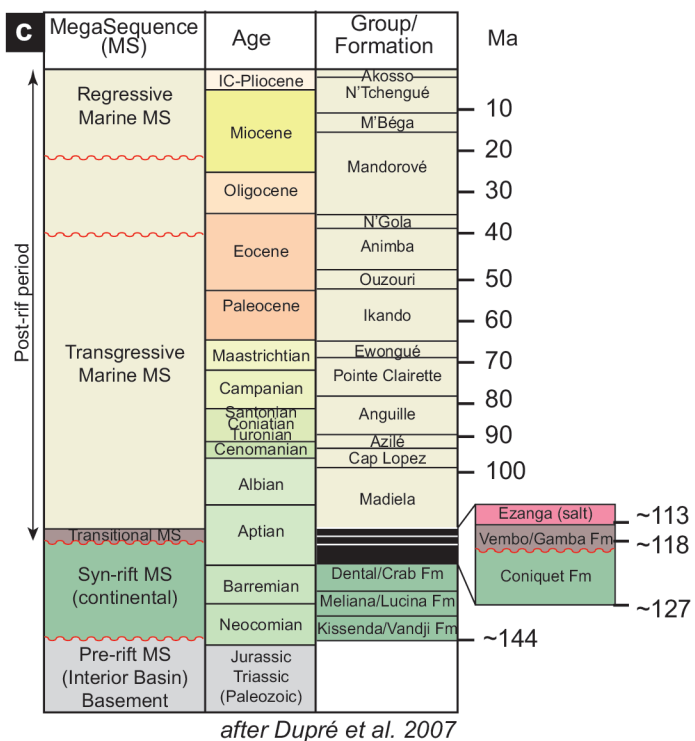
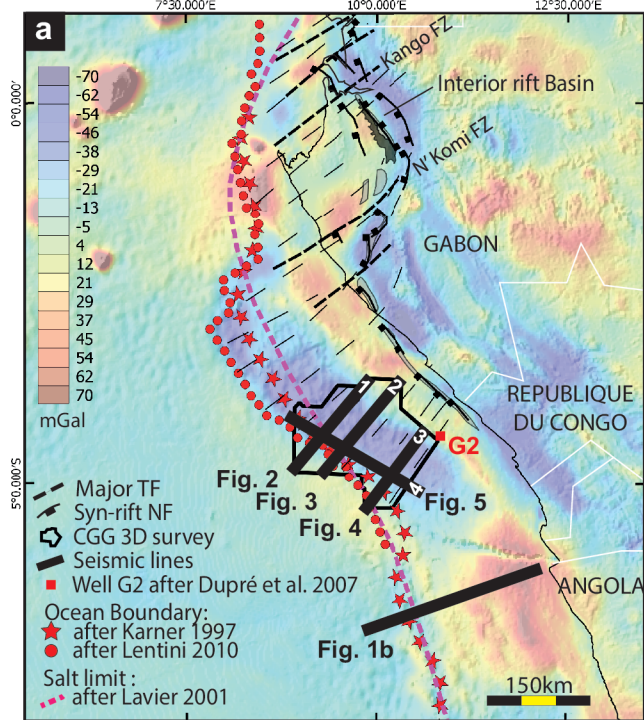
- Beslier, M.-O., Royer, J.-Y., Girardeau, J., Hill, P. J., Boeuf, E., Buchanan, C., Chatin, F., Jacovetti, G., Moreau, A., & Munsch, M. (2004). Une large transition continent-ocean en pied de marge sud-ouest australienne: premiers resultats de la campagne MARGAU/MD110. *Bulletin de la Société géologique de France*, 175(6), 629-641.
- Bonatti, E. (1985). Punctiform initiation of seafloor spreading in the Red Sea during transition from a continental to an oceanic rift. *Nature*, 316(6023), 33-37.
- Brink, A. H. (1974). Petroleum geology of Gabon Basin. *AAPG Bulletin*, 58, 216-235.
- Brune, S., Heine, C., Clift, P. D., & Pérez-Gussinyé, M. (2017). Rifted margin architecture and crustal rheology: reviewing Iberia-Newfoundland, central South Atlantic, and South China Sea. *Marine and Petroleum Geology*, 79, 257-281.
- Brune, S., Heine, C., Pérez-Gussinyé, M., & Sobolev, S. V. (2014). Rift migration explains continental margin asymmetry and crustal hyper-extension. *Nature Communications*, 5(1), 1-9.
- Charpentier, S., Kornprobst, J., Chazot, G., Cornen, G., & Boillot, G. (1998). Interaction entre lithosphère et asthénosphère au cours de l'ouverture océanique: données isotopiques préliminaires sur la Marge passive de Galice (Atlantique-Nord). *Comptes Rendus de l'Académie des Sciences-Series IIA-Earth and Planetary Science*, 326(11), 757-762.
- Chauvet, F., Sapin, F., Geoffroy, L., Ringenbach, J. C., & Ferry, J. N. (2020). Conjugate volcanic passive margins in the austral segment of the South Atlantic—Architecture and development. *Earth-Science Reviews*, 103461.
- Clerc, C., Ringenbach, J. C., Jolivet, L., & Ballard, J. F. (2018). Rifted margins: Ductile deformation, boudinage, continentward-dipping normal faults and the role of the weak lower crust. *Gondwana Research*, 53, 20-40.
- Cowie, L., Angelo, R., Kuszniir, N., Manatschal, G., & Horn, B. (2016). The palaeo-bathymetry of base Aptian salt deposition on the northern Angolan rifted margin: constraints from flexural back-stripping and reverse post-break-up thermal subsidence modelling. *Petroleum Geoscience*, 22(1), 59-70.
- Curry, M. A., Peel, F. J., Hudec, M. R., & Norton, I. O. (2018). Extensional models for the development of passive-margin salt basins, with application to the Gulf of Mexico. *Basin Research*, 30(6), 1180-1199.
- Davison, I. (1999). Tectonics and hydrocarbon distribution along the Brazilian South Atlantic margin. *Geological Society, London, Special Publications*, 153(1), 133-151.
- Davison, I. (2007). Geology and tectonics of the South Atlantic Brazilian salt basins. *Geological Society, London, Special Publications*, 272(1), 345-359.
- Debure, M., Lassin, A., Marty, N. C., Claret, F., Virgone, A., Calassou, S., & Gaucher, E. C. (2019). Thermodynamic evidence of giant salt deposit formation by serpentinization: an alternative mechanism to solar evaporation. *Scientific reports*, 9(1), 1-11.
- Dick, H. J., Lin, J., & Schouten, H. (2003). An ultraslow-spreading class of ocean ridge. *Nature*, 426(6965), 405-412.
- Ding, W., Li, J., Clift, P. D., & Expedition, I. (2016). Spreading dynamics and sedimentary process of the Southwest Sub-basin, South China Sea: constraints from multi-channel seismic data and IODP Expedition 349. *Journal of Asian Earth Sciences*, 115, 97-113.

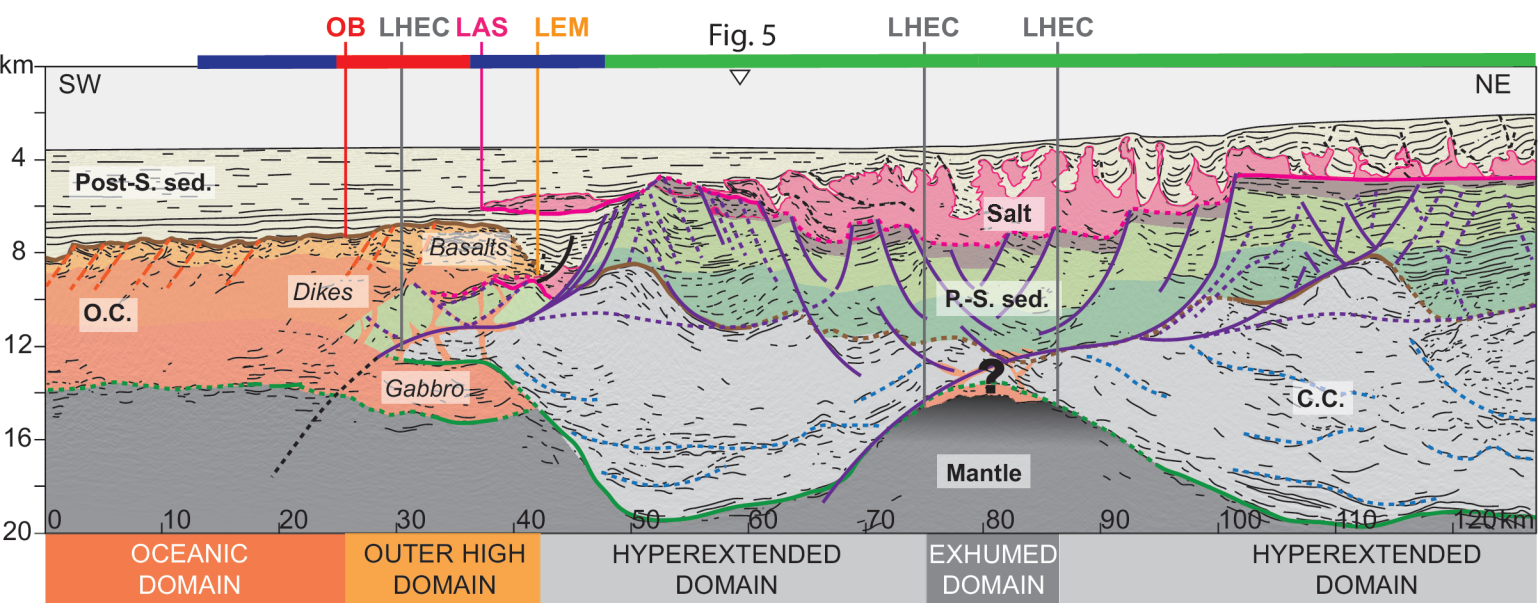
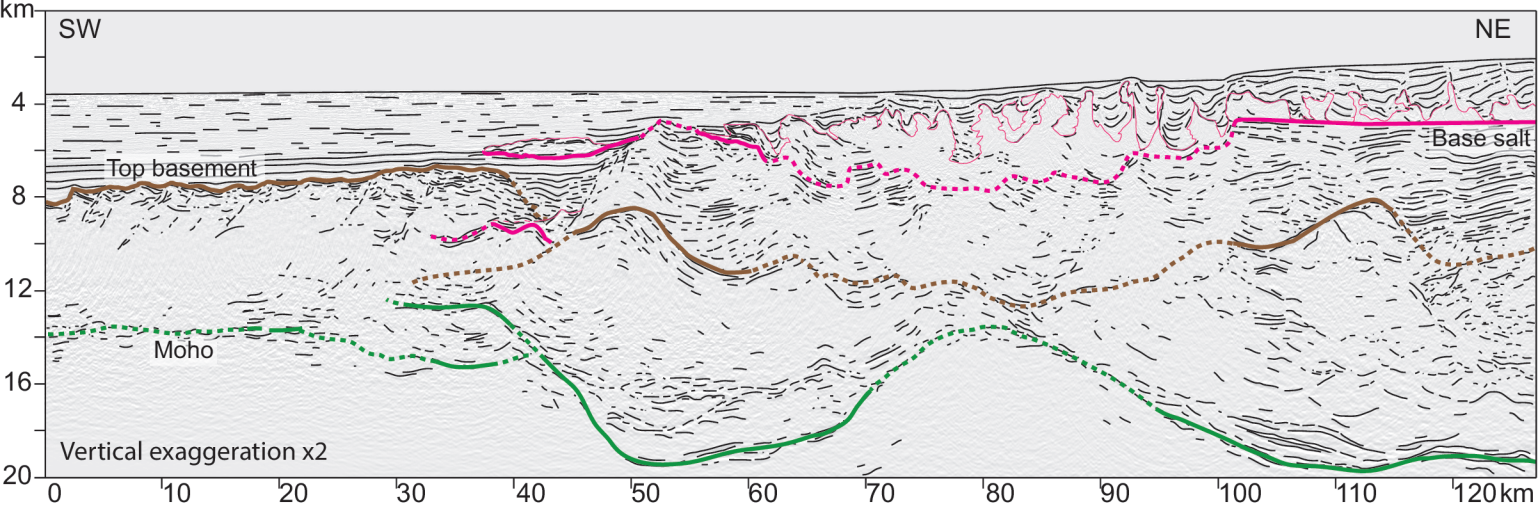
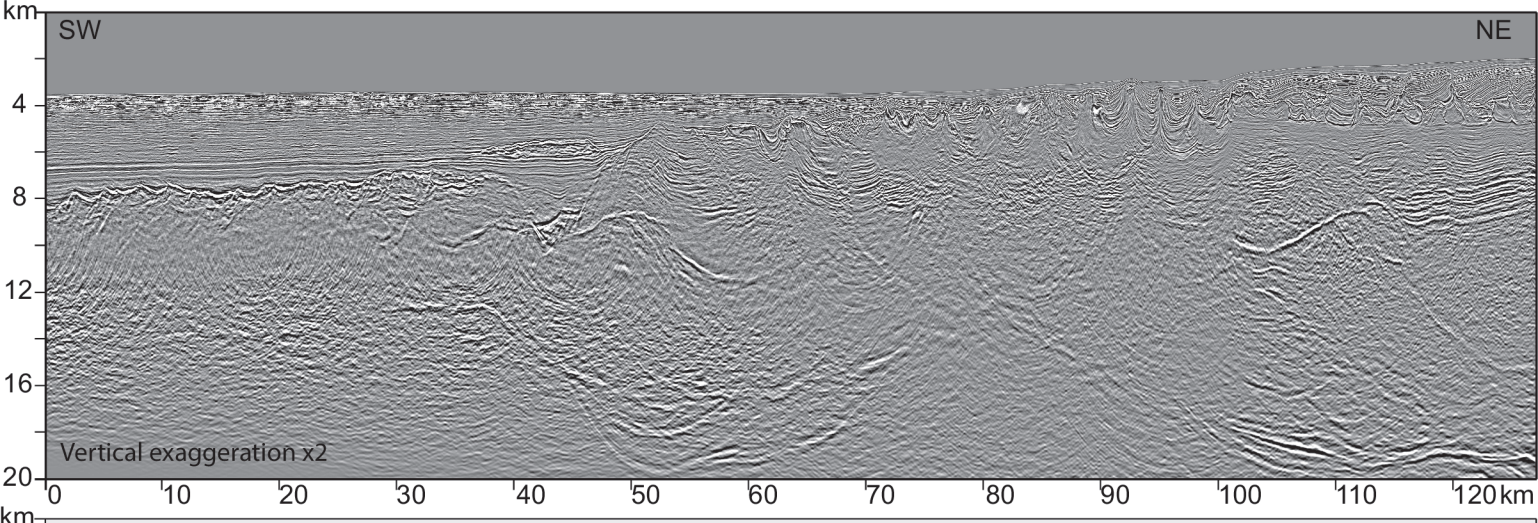
- Dupré, S., Bertotti, G., & Cloetingh, S. (2007). Tectonic history along the South Gabon Basin: anomalous early post-rift subsidence. *Marine and Petroleum Geology*, 24(3), 151-172.
- Duran, P. M., Pearsons, M., Soyer, W., & Duval, G. (2018). Evidence for a More Complex Crustal Setting Offshore Gabon: Support from a High-Resolution Regional Seismic Dataset Int. *Paper presented at the 80th EAGE Conference and Exhibition 2018*.
- Duval, G., & Firth, J. (2015). G&G integration enhances acquisition of multi-client studies offshore Gabon. *World Oil*, 57-61.
- Epin, M.-E., Manatschal, G., Amman, M., Ribes, C., Clause, A., Guffon, T., & Lescanne, M. (2019). Polyphase tectono-magmatic evolution during mantle exhumation in an ultra-distal, magma-poor rift domain: example of the fossil Platta ophiolite, SE Switzerland. *International Journal of Earth Sciences*, 1-25.
- Fernandez, O., Olaiz, A., Cascone, L., Hernandez, P., de Faria, A., Tritlla, J., Ingles, M., Aida, B., Pinto, I., & Rocca, R. (2020). Geophysical evidence for breakup volcanism in the Angola and Gabon passive margins. *Marine and Petroleum Geology*, 104330.
- Gillard, M., Autin, J., Manatschal, G., Sauter, D., Munsch, M., & Schaming, M. (2015). Tectonomagmatic evolution of the final stages of rifting along the deep conjugate Australianthe Angola and Gabon passive margins. e fosaursints from seismic observations. *Tectonics*, 34(4), 753-783.
- Gillard, M., Sauter, D., Tugend, J., Tomasi, S., Epin, M.-E., & Manatschal, G. (2017). Birth of an oceanic spreading center at a magma-poor rift system. *Scientific reports*, 7(1), 1-6.
- Gillard, M., Tugend, J., Müntener, O., Manatschal, G., Karner, G. D., Autin, J., ... & Ulrich, M. (2019). The role of serpentinization and magmatism in the formation of decoupling interfaces at magma-poor rifted margins. *Earth-Science Reviews*, 196, 102882.
- Gładczenko, T., Hinz, K., Eldholm, O., Meyer, H., Neben, S., & Skogseid, J. (1997). South Atlantic volcanic margins. *Journal of the Geological Society*, 154(3), 465-470.
- Guiraud, R., & Maurin, J.-C. (1991). Le Rifting en Afrique au Cretace inferieur; synthese structurale, mise en evidence de deux etapes dans la genese des bassins, relations avec les ouvertures oceaniques peri-africaines. *Bulletin de la Société géologique de France*, 162(5), 811-823.
- Heine, C., Zoethout, J., & Müller, R. D. (2013). Kinematics of the South Atlantic rift. arXiv preprint arXiv:1301.2096.
- Hossack, J. (1995). Geometric rules of section balancing for salt structures, in M.P.A. Jackson, D.G. Roberts, and S. Snelson, eds., Salt tectonics: a global perspective. *AAPG Memoir*, 65, 29-40.
- Howe, J. A., Stoker, M. S., & Woolfe, K. J. (2001). Deep-marine seabed erosion and gravel lags in the northwestern Rockall Trough, North Atlantic Ocean. *Journal of the Geological Society*, 158, 427-438.
- Hudec, M. R., Dooley, T. P., Peel, F. J., & Soto, J. I. (2020). Controls on the evolution of passive-margin salt basins: Structure and evolution of the Salina del Bravo region, northeastern Mexico. *Bulletin*, 132(5-6), 997-1012.
- Karner, G., & Gambôa, L. (2007). Timing and origin of the South Atlantic pre-salt sag basins and their capping evaporites. *Geological Society, London, Special Publications*, 285(1), 15-35.

- Karner, G. D., Driscoll, N. W., McGinnis, J. P., Brumbaugh, W. D., & Cameron, N. R. (1997). Tectonic significance of syn-rift sediment packages across the Gabon-Cabinda continental margin. *Marine and Petroleum Geology*, 14(7-8), 973-1000.
- Larsen, H. C., Mohn, G., Nirrengarten, M., Sun, Z., Stock, J., Jian, Z., Klaus, A., Alvarez-Zarikian, C., Boaga, J., & Bowden, S. (2018). Rapid transition from continental breakup to igneous oceanic crust in the South China Sea. *Nature Geoscience*, 11(10), 782-789.
- Lavier, L., Ball, P., Manatschal, G., Heumann, M., MacDonald, J., Matt, V., & Schneider, C. (2019). Controls on the Thermomechanical Evolution of Hyperextended Lithosphere at Magma-Poor Rifted Margins: The Example of Espirito Santo and the Kwanza Basins. *Geochemistry, Geophysics, Geosystems*, 20(11), 5148-5176.
- Lavier, L. L., Steckler, M. S., & Brigaud, F. (2001). Climatic and tectonic control on the Cenozoic evolution of the West African margin. *Marine Geology*, 178(1-4), 63-80.
- Lentini, M. R., Fraser, S. I., Sumner, H. S., & Davies, R. J. (2010). Geodynamics of the central South Atlantic conjugate margins: implications for hydrocarbon potential. *Petroleum Geoscience*, 16(3), 217-229.
- Ligi, M., Bonatti, E., Bosworth, W., Cai, Y., Cipriani, A., Palmiotto, C., Ronca, S., & Seyler, M. (2018). Birth of an ocean in the Red Sea: Oceanic-type basaltic melt intrusions precede continental rupture. *Gondwana Research*, 54, 150-160.
- Lymer, G., Cresswell, D. J., Reston, T. J., Bull, J. M., Sawyer, D. S., Morgan, J. K., Stevenson, C., Causer, A., Minshull, T. A., & Shillington, D. J. (2019). 3D development of detachment faulting during continental breakup. *Earth and Planetary Science Letters*, 515, 90-99.
- Manatschal, G., Lavier, L., & Chenin, P. (2015). The role of inheritance in structuring hyperextended rift systems: Some considerations based on observations and numerical modeling. *Gondwana Research*, 27(1), 140-164.
- Manatschal, G., & Müntener, O. (2009). A type sequence across an ancient magma-poor ocean-continent transition: the example of the western Alpine Tethys ophiolites. *Tectonophysics*, 473(1-2), 4-19.
- Meyers, J. B., Rosendahl, B. R., & Jr, J. A. (1996). Deep-penetrating MCS images of the South Gabon Basin: implications for rift tectonics and post-breakup salt remobilization. *Basin Research*, 8(1), 65-84.
- Mohn, G., Manatschal, G., Beltrando, M., Masini, E., & Kuszniir, N. (2012). Necking of continental crust in magmalites. mple oftonics and post-breakup salt remobilization. modeling. *Tectonics*, 31(1).
- Moulin, M., Aslanian, D., Olivet, J.-L., Contrucci, I., Matias, L., Géli, L., Klingelhoefer, F., Nouzé, H., Réhault, J.-P., & Unternehr, P. (2005). Geological constraints on the evolution of the Angolan margin based on reflection and refraction seismic data (ZaïAngo project). *Geophysical Journal International*, 162(3), 793-810.
- Moulin, M., Aslanian, D., & Unternehr, P. (2010). A new starting point for the South and Equatorial Atlantic Ocean. *Earth-Science Reviews*, 98(1-2), 1-37.
- Moulin, M., Klingelhoefer, F., Afilhado, A., Aslanian, D., Schnurle, P., Nouzé, H., ... & Feld, A. (2015). Deep crustal structure across a young passive margin from wide-angle and reflection

- seismic data (The SARDINIA Experiment)–I. Gulf of Lion's margin. *Bulletin de la Société géologique de France*, 186(4-5), 309-330.
- Mounguengui, M. M., & Guiraud, M. (2009). Neocomian to early Aptian syn-rift evolution of the normal to oblique-rifted North Gabon Margin (Interior and N'Komi Basins). *Marine and Petroleum Geology*, 26(6), 1000-1017.
- Nirrengarten, M., Mohn, G., Schito, A., Corrado, S., Gutiérrez-García, L., Bowden, S. A., & Despinois, F. (2020). The thermal imprint of continental breakup during the formation of the South China Sea. *Earth and Planetary Science Letters*, 531, 115972.
- Norton, I. O., Carruthers, D. T., & Hudec, M. R. (2016). Rift to drift transition in the South Atlantic salt basins: A new flavor of oceanic crust. *Geology*, 44(1), 55-58.
- Norton, I. O., Van Avendonk, H. J., Christeson, G. L., & Eddy, D. R. (2014). Formation of the Gulf of Mexico Salt Basin. *AGUFM, 2014*, T53B-4682.
- Parsons, M., Duran, P. M., Soyer, W., & Duval, G. (2017). Understanding the tectonic history offshore Southern Gabon with high resolution seismic, gravity and magnetics. *First Break*, 35(9), 81-87.
- Péron-Pinvidic, G., & Manatschal, G. (2010). From microcontinents to extensional allochthons: witnesses of how continents rift and break apart? *Petroleum Geoscience*, 16(3), 189-197.
- Péron-Pinvidic, G., Manatschal, G., Masini, E., Sutra, E., Flament, J. M., Hauptert, I., & Unternehr, P. (2017). Unravelling the along-strike variability of the Angola–Gabon rifted margin: a mapping approach. *Geological Society, London, Special Publications*, 438(1), 49-76.
- Péron-Pinvidic, G., Manatschal, G., Minshull, T. A., & Sawyer, D. S. (2007). Tectonosedimentary evolution of the deep Iberia-Newfoundland margins: Evidence for a complex breakup history. *Tectonics*, 26(2).
- Péron-Pinvidic, G., Manatschal, G., & Osmundsen, P. T. (2013). Structural comparison of archetypal Atlantic rifted margins: A review of observations and concepts. *Marine and Petroleum Geology*, 43, 21-47.
- Péron-Pinvidic, G., & Osmundsen, P. T. (2016). Architecture of the distal and outer domains of the Mid-Norwegian rifted margin: Insights from the Rån-Gjallar ridges system. *Marine and Petroleum Geology*, 77, 280-299.
- Pindell, J., Graham, R., & Horn, B. (2014). Rapid outer marginal collapse at the rift to drift transition of passive margin evolution, with a Gulf of Mexico case study. *Basin Research*, 26(6), 701-725.
- Reston, T. J. (2010). The opening of the central segment of the South Atlantic: symmetry and the extension discrepancy. *Petroleum Geoscience*, 16(3), 199-206.
- Ribes, C., Manatschal, G., Ghienne, J.-F., Karner, G. D., Johnson, C. A., Figueredo, P. H., Incerpi, N., & Epin, M.-E. (2019). The syn-rift stratigraphic record across a fossil hyper-extended rifted margin: the example of the northwestern Adriatic margin exposed in the Central Alps. *International Journal of Earth Sciences*, 108(6), 2071-2095.
- Rowan, M. G. (2018). The South Atlantic and Gulf of Mexico salt basins: crustal thinning, subsidence and accommodation for salt and presalt strata. *Geological Society, London, Special Publications*, 476, SP476. 476.

- Rowan, M. G., & Jarvie, A. (2020). Crustal extension and salt tectonics of the Danmarkshavn Ridge and adjacent basins, NE Greenland. *Marine and Petroleum Geology*, 104339.
- Ryan, W. B. (2009). Decoding the Mediterranean salinity crisis. *Sedimentology*, 56, 95-136.
- Saller, A., Rushton, S., Buambua, L., Inman, K., McNeil, R., & Dickson, J. A. D. (2016). Presalt stratigraphy and depositional systems in the Kwanza Basin, offshore Angola. *AAPG Bulletin*, 100, 1135-1164.
- Sandwell, D. T., Müller, R. D., Smith, W. H., Garcia, E., & Francis, R. (2014). New global marine gravity model from CryoSat-2 and Jason-1 reveals buried tectonic structure. *Science*, 346(6205), 65-67.
- Sapin, F., Ringenbach J.-C., Clerc C. (accepted). Rifted margins classification and forcing parameters. *Nature Scientific Reports*.
- Stanton, N., Manatschal, G., Autin, J., Sauter, D., Maia, M., & Viana, A. (2016). Geophysical fingerprints of hyper-extended, exhumed and embryonic oceanic domains: the example from the Iberia–Newfoundland rifted margins. *Marine Geophysical Research*, 37(3), 185-205.
- Stica, J. M., Zalán, P. V., & Ferrari, A. L. (2014). The evolution of rifting on the volcanic margin of the Pelotas Basin and the contextualization of the Paraná–Etendeka LIP in the separation of Gondwana in the South Atlantic. *Marine and Petroleum Geology*, 50, 1-21.
- Sutra, E., Manatschal, G., Mohn, G., & Unternehr, P. (2013). Quantification and restoration of extensional deformation along the Western Iberia and Newfoundland rifted margins. *Geochemistry, Geophysics, Geosystems*, 14(8), 2575-2597.
- Szameitat, L. S., Manatschal, G., Nirrengarten, M., Ferreira, F. J., & Heilbron, M. (2020). Magnetic characterization of the zigzag shaped J-anomaly: Implications for kinematics and breakup processes at the Iberia–Newfoundland margins. *Terra Nova*, 32(5), 369-380.
- Teisserenc, P., & Villemin, J. (1990). Sedimentary basin of Gabon : geology and oil systems : *AAPG Memoir*, 48, 117-199.
- Torsvik, T. H., Rousse, S., Labails, C., & Smethurst, M. A. (2009). A new scheme for the opening of the South Atlantic Ocean and the dissection of an Aptian salt basin. *Geophysical Journal International*, 177(3), 1315-1333.
- Tugend, J., Gillard, M., Manatschal, G., Nirrengarten, M., Harkin, C., Epin, M. E., ... & Mcdermott, K. (2020). Reappraisal of the magma-rich versus magma-poor rifted margin archetypes. *Geological Society, London, Special Publications*, 476(1), 23-47.
- Tugend, J., Manatschal, G., & Kusznir, N. (2015). Spatial and temporal evolution of hyperextended rift systems: Implication for the nature, kinematics, and timing of the Iberian-European plate boundary. *Geology*, 43(1), 15-18.
- Tugend, J., Manatschal, G., Kusznir, N., Masini, E., Mohn, G., & Thinon, I. (2014). Formation and deformation of hyperextended rift systems: Insights from rift domain mapping in the Bay of Biscay-Pyrenees. *Tectonics*, 33(7), 1239-1276.
- Weaver, P. P. E., & Thomson, J. (1993). Calculating erosion by deep-sea turbidity currents during initiation and flow. *Nature*, 364, 136-138.



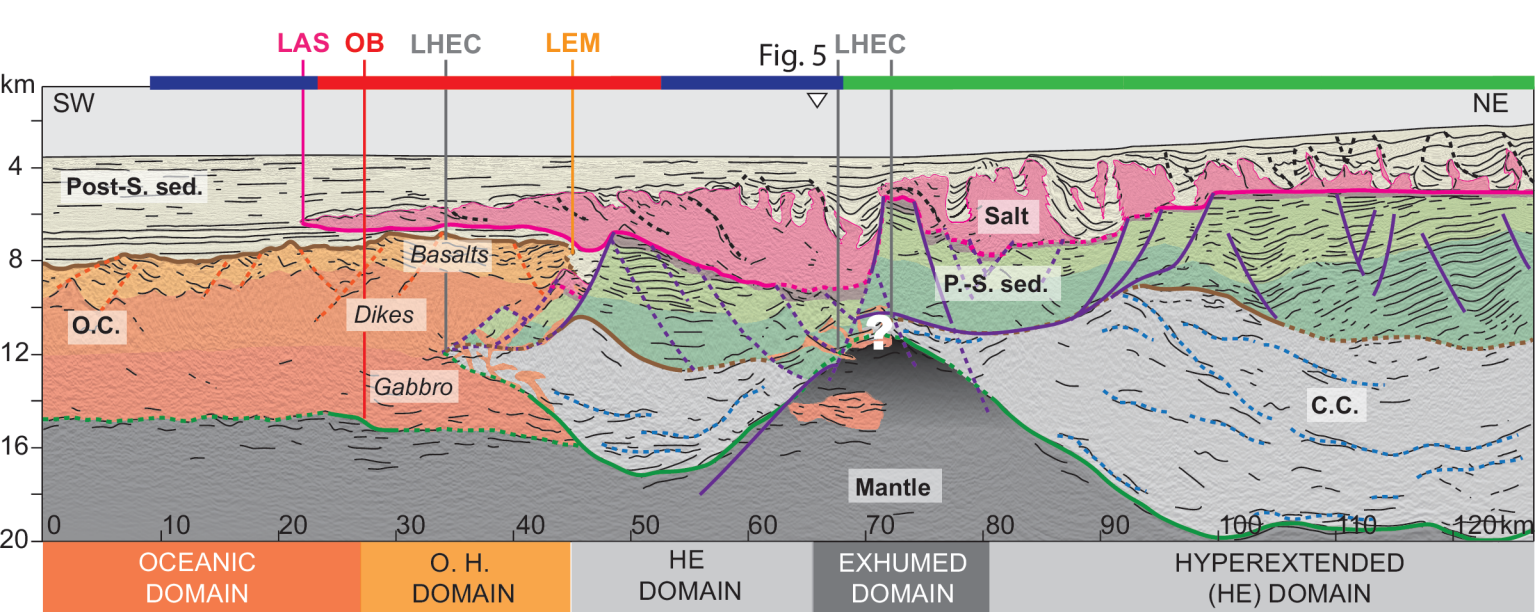
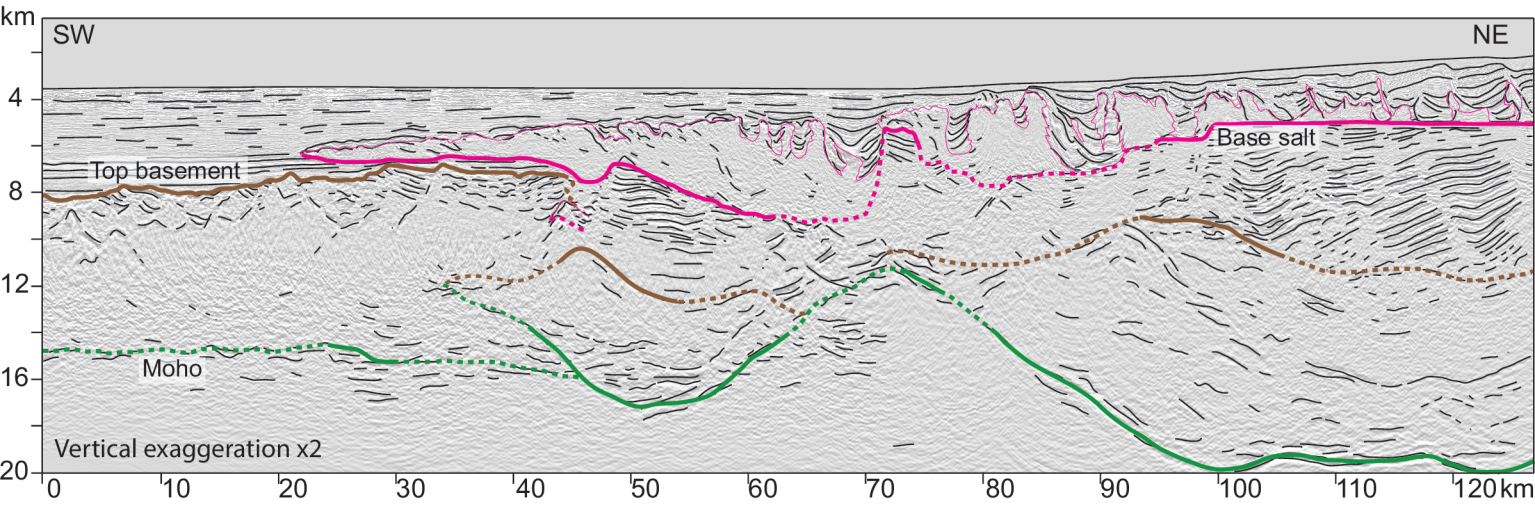
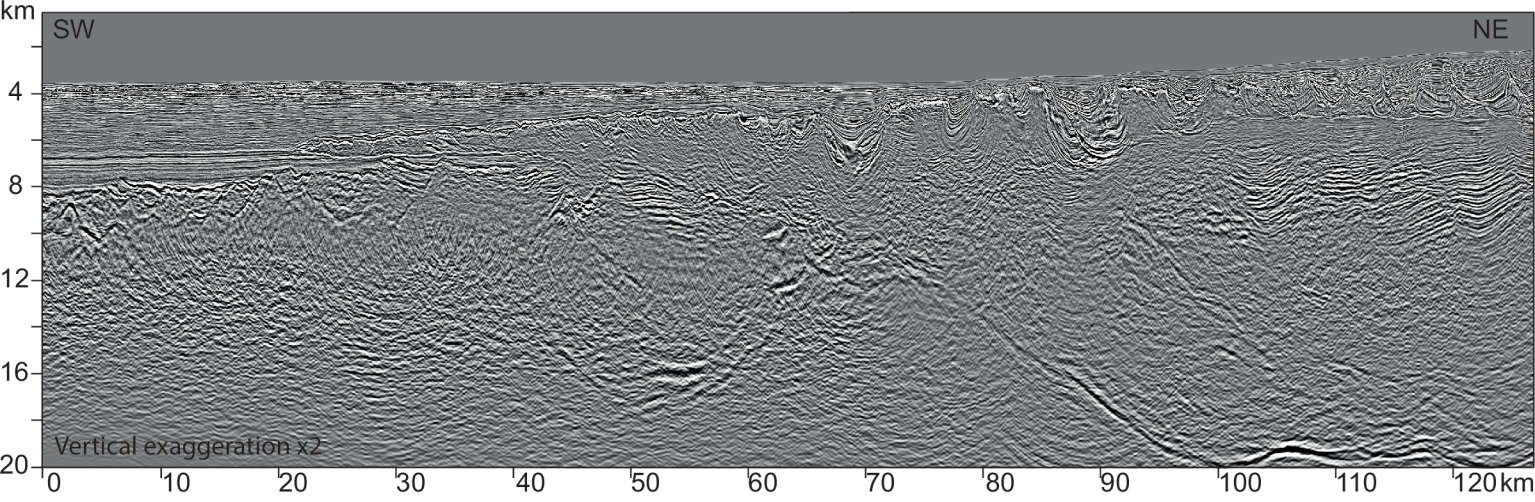


- Post-salt sediments (Post-S. sed.)
- Salt
- Pre-salt sediments (P-S. sed.)
- Continental crust (C.C.)
- Lithospheric mantle
- Serpentinization front

- Oceanic crust (O.C.)
- Extrusive magmatism - Basalts
- Dikes - Sheeted dike
- Intrusive magmatism - Gabbro
- Base salt
- Top basement
- Moho

- Fault generation
- Simplified profile from dRTP Magnetic (nT) map, after Parsons et al. 2017, see Fig. 6 for scale

OB: Ocean Boundary; LAS: Limit of Allochthonous Salt; LEM: Limit of Extrusive Magmatism; LHEX: Limit of Hyperextended Continental crust

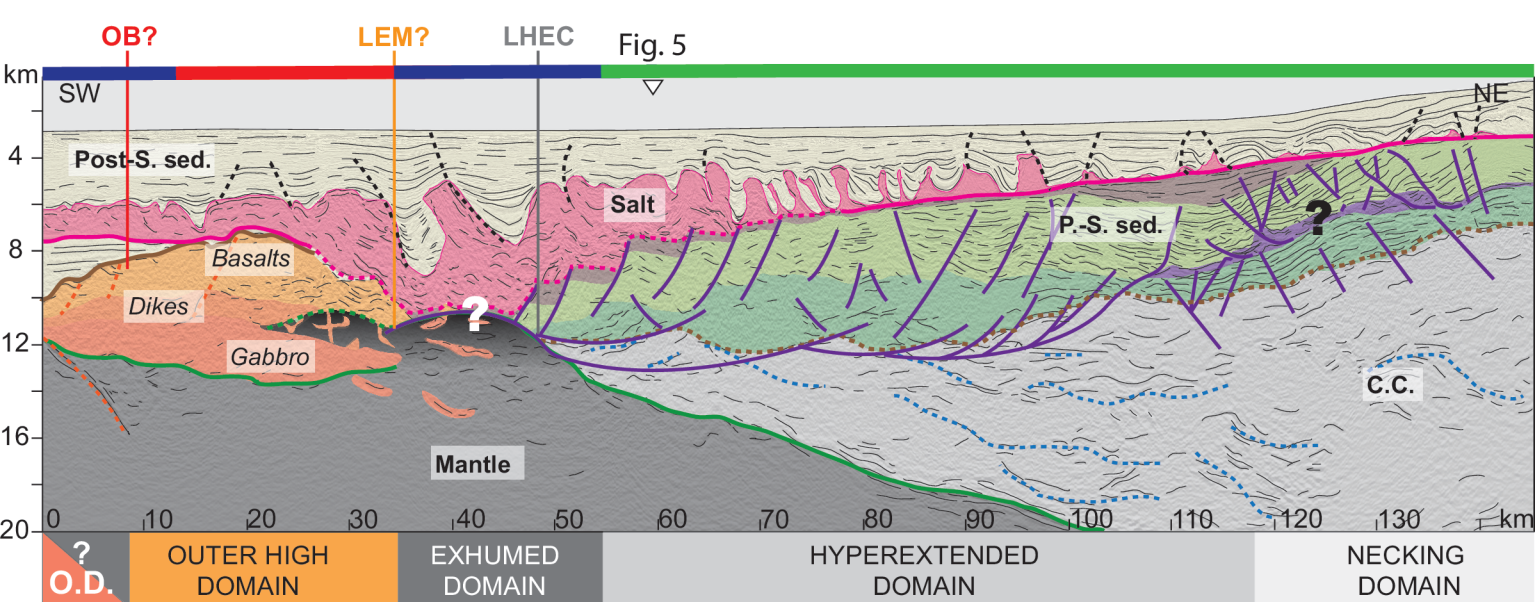
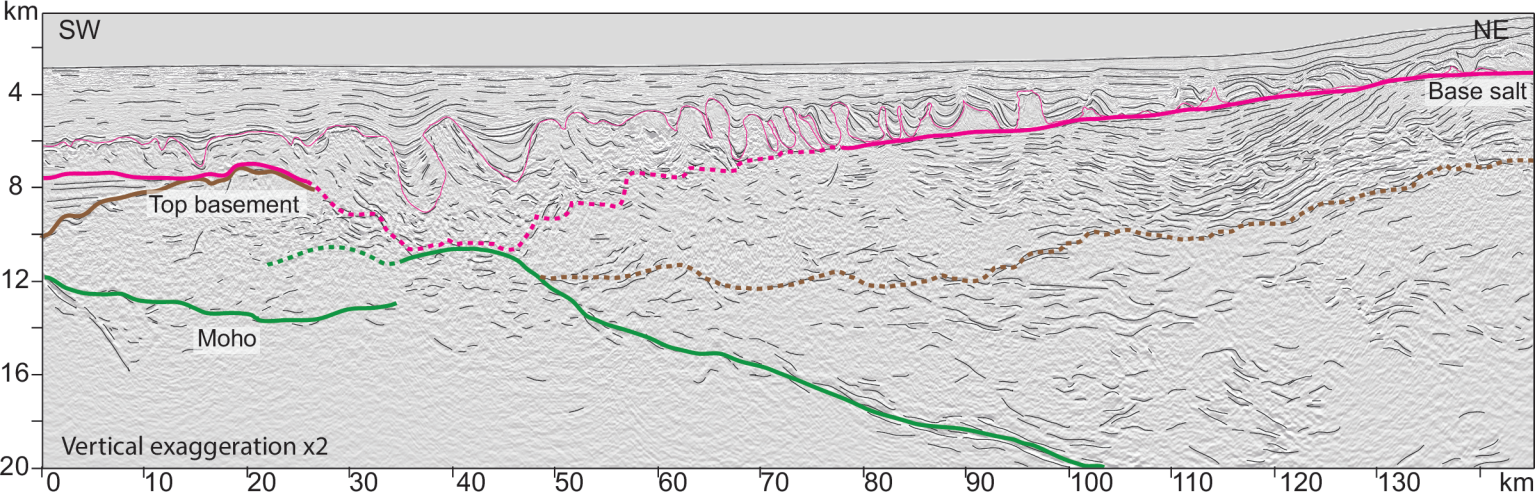
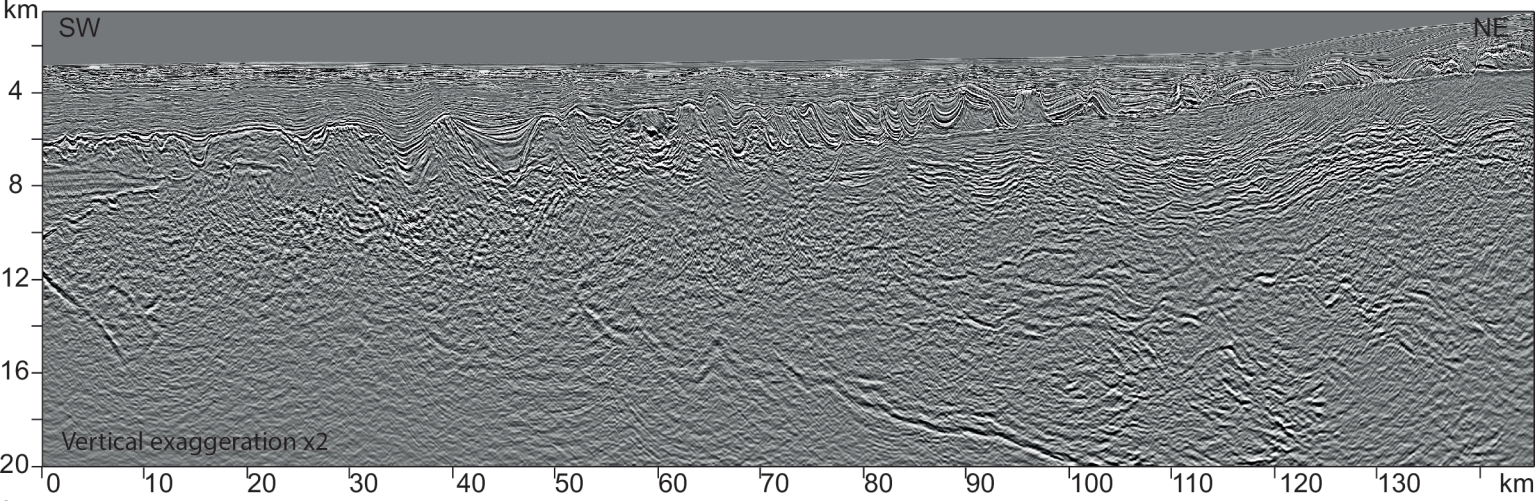


■ Post-salt sediments (Post-S. sed.)
 ■ Salt
 ■ Pre-salt sediments (P.-S. sed.)
 ■ Continental crust (C.C.)
 ■ Lithospheric mantle
 ■ Serpentinization front

Oceanic crust (O.C.)
 ■ Extrusive magmatism - Basalts
 ■ Dikes - Sheeted dike
 ■ Intrusive magmatism - Gabbro
 ■ Base salt
 ■ Top basement
 ■ Moho

■ Fault generation
 ■ Simplified profile from dRTP Magnetic (nT) map, after Parsons et al. 2017, see Fig. 6 for scale

OB: Ocean Boundary; LAS: Limit of Allochthonous Salt; LEM: Limit of Extrusive Magmatism; LHEC: Limit of Hyperextended Continental crust; O.H. : Outer High domain



Post-salt sediments (Post-S. sed.)

Salt

Pre-salt sediments (P.-S. sed.)

Continental crust (C.C.)

Lithospheric mantle

Serpentinization front

Oceanic crust (O.C.)

Extrusive magmatism - Basalts

Dikes - Sheeted dike

Intrusive magmatism - Gabbro

Base salt

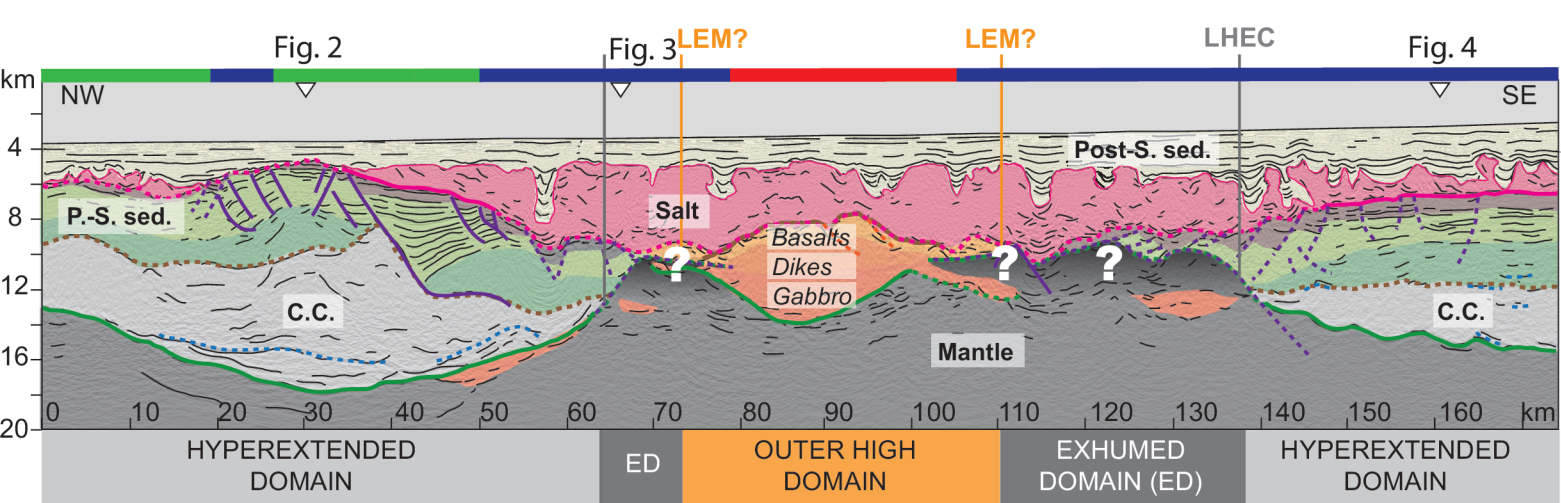
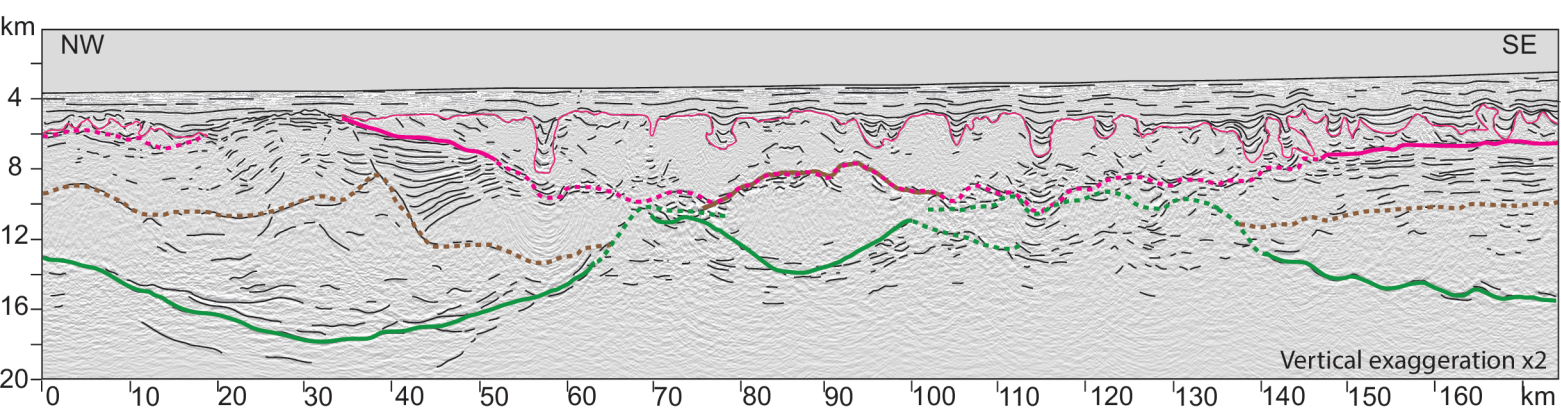
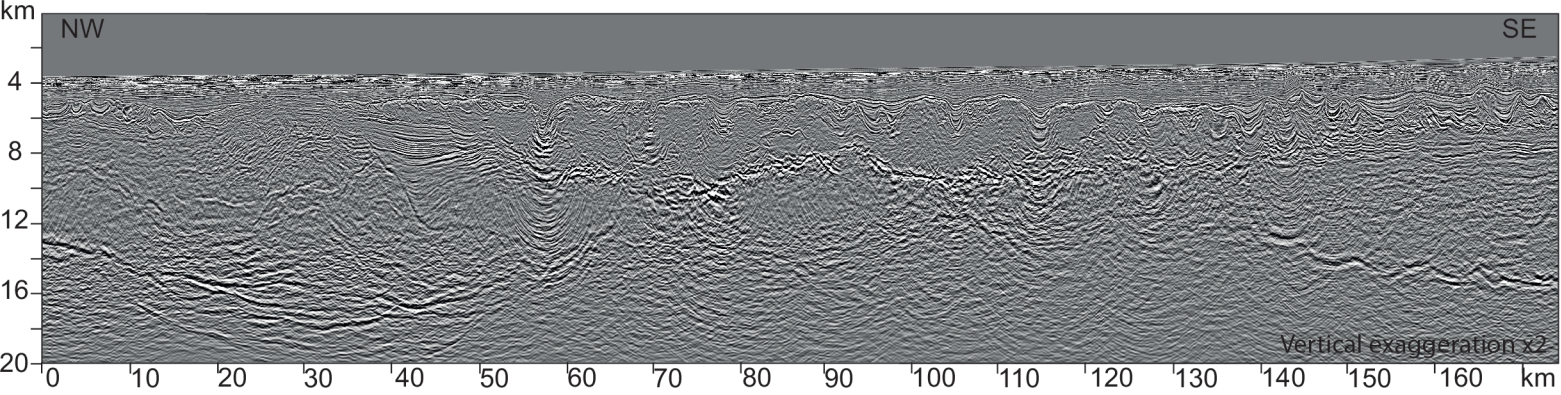
Top basement

Moho

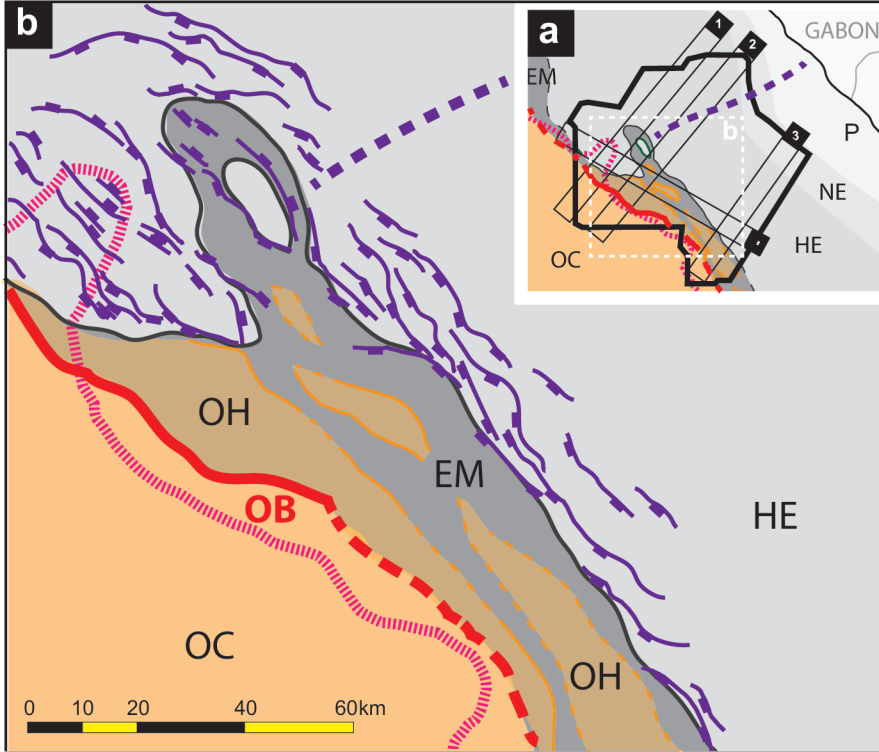
Fault generation

Simplified profile from dRTP Magnetic (nT) map, after Parsons et al. 2017, see Fig. 6 for scale

OB: Ocean Boundary; LEM: Limit of Extrusive Magmatism; LHEC: Limit of Hyperextended Continental crust; O.D.: Oceanic domain



LHEC: Limit of Hyperextended Continental crust; LEM: Limit of Extrusive Magmatism



Legende

- P Continental crust
- NE Continental crust
- HE Continental crust
- EM Lithospheric mantle
- OH Extrusive magmatism
- OB** Ocean boundary
- Limit of allochthonous salt
- OC Oceanic crust
- Major violet faults
- Boundary between north and south

P: Proximal domain

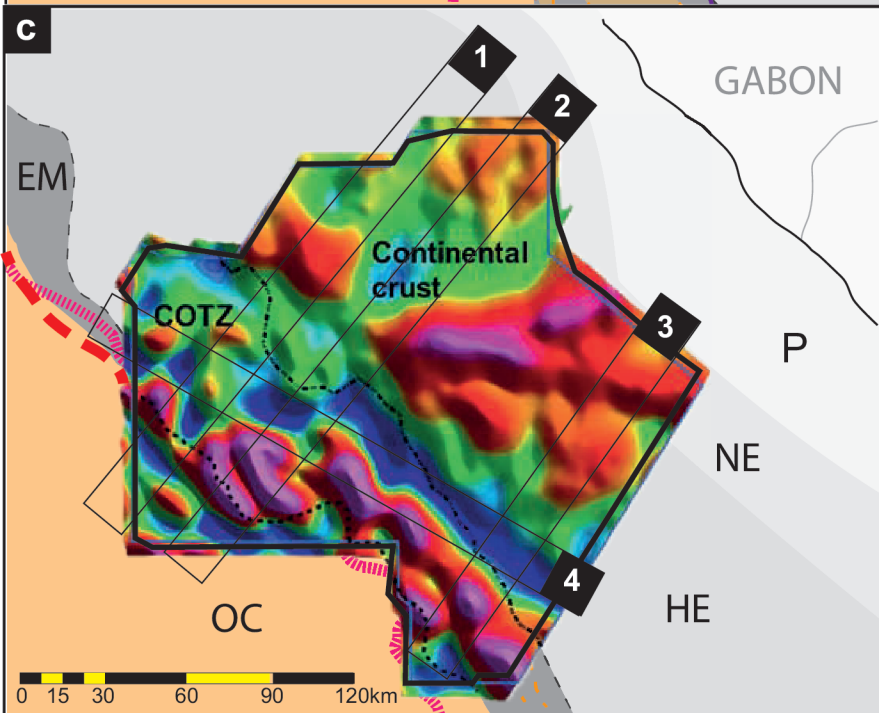
NE: Necking domain

HE: Hyper-Extended domain

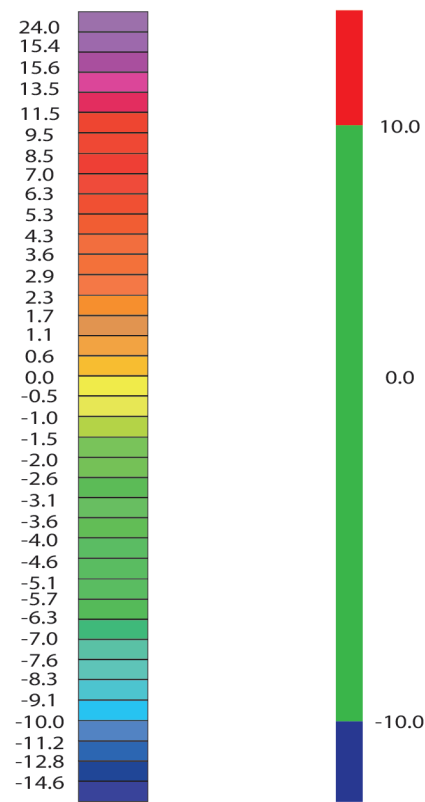
EM: Exhumed Mantle domain

OH: Outer High

OC: Oceanic Crust

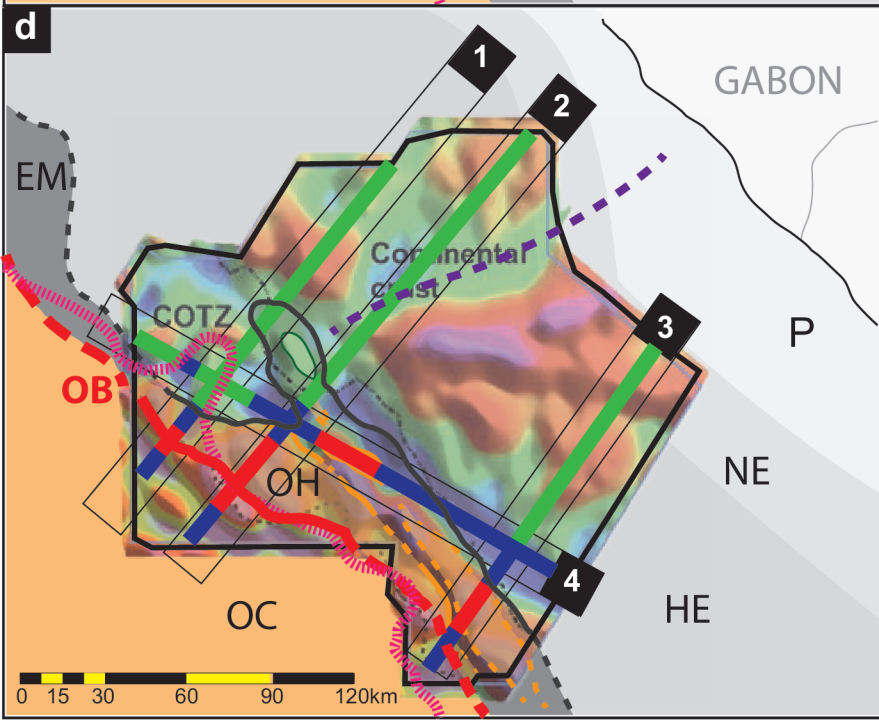


dRTP Magnetics map
after Parsons et al. 2017



Matched filter ~9km
dRTP Magnetic (nT)

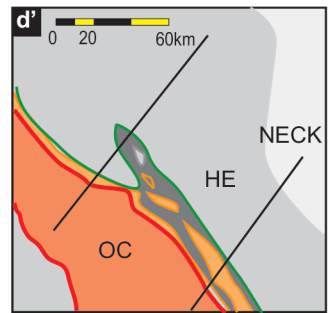
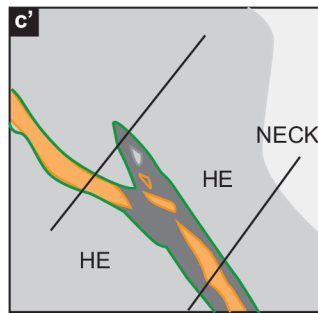
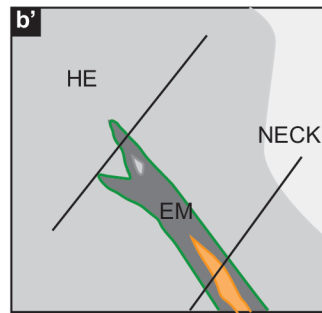
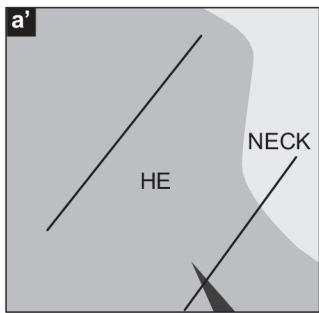
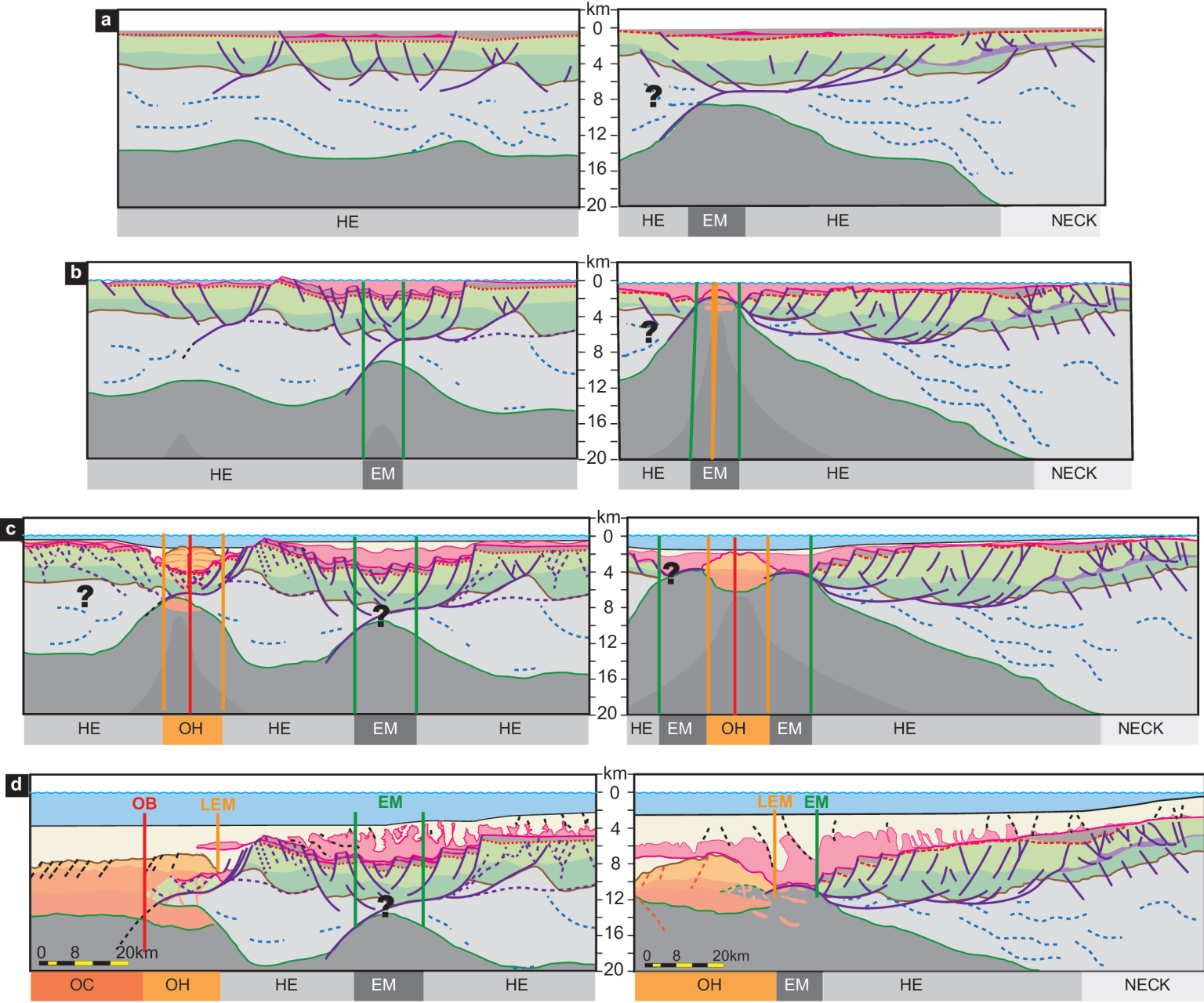
Simplified
dRTP Magnetic (nT)



Continent Ocean Transition (COT) Zone
after Parsons et al. 2017

- COT Inner bound
- COT Outer bound

EVOLUTION OF THE NORTHERN PART

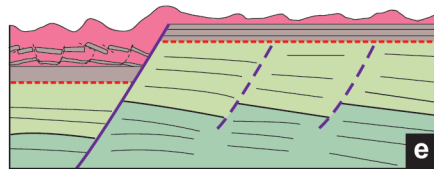
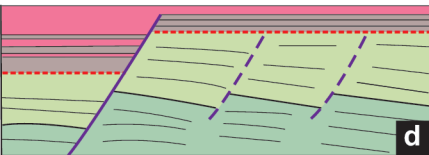
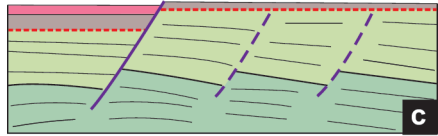
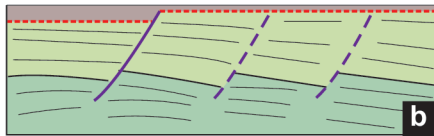
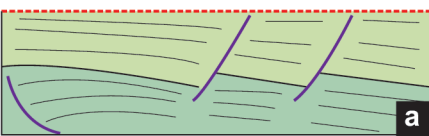






OB: Ocean Boundary; LEM: Limit of Extrusive Magmatism; LAS: Limit of Allochthonous salt; LautoS: Limit of Autochthonous Salt; EM: Exhumed Mantle domain; HE: Hyper-extended domain; OH: Outer High domain; POC: Proto-Oceanic Domain; OC: Oceanic Crust; NECK: Necking domain

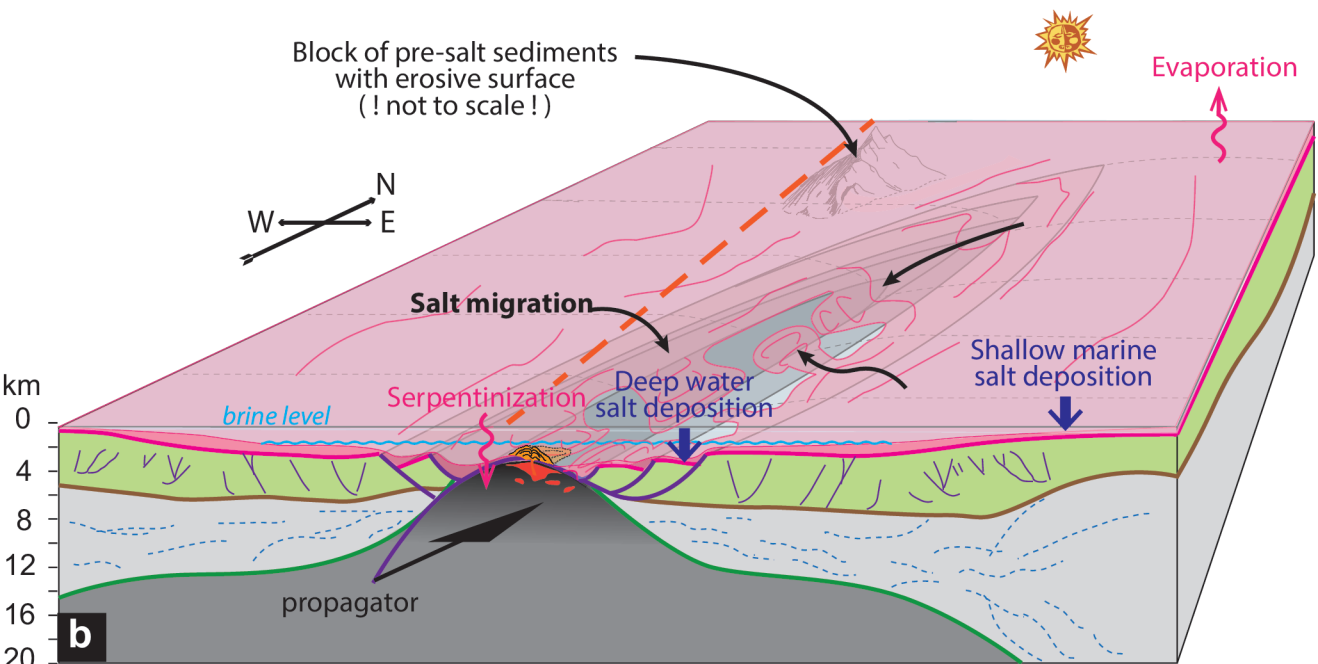
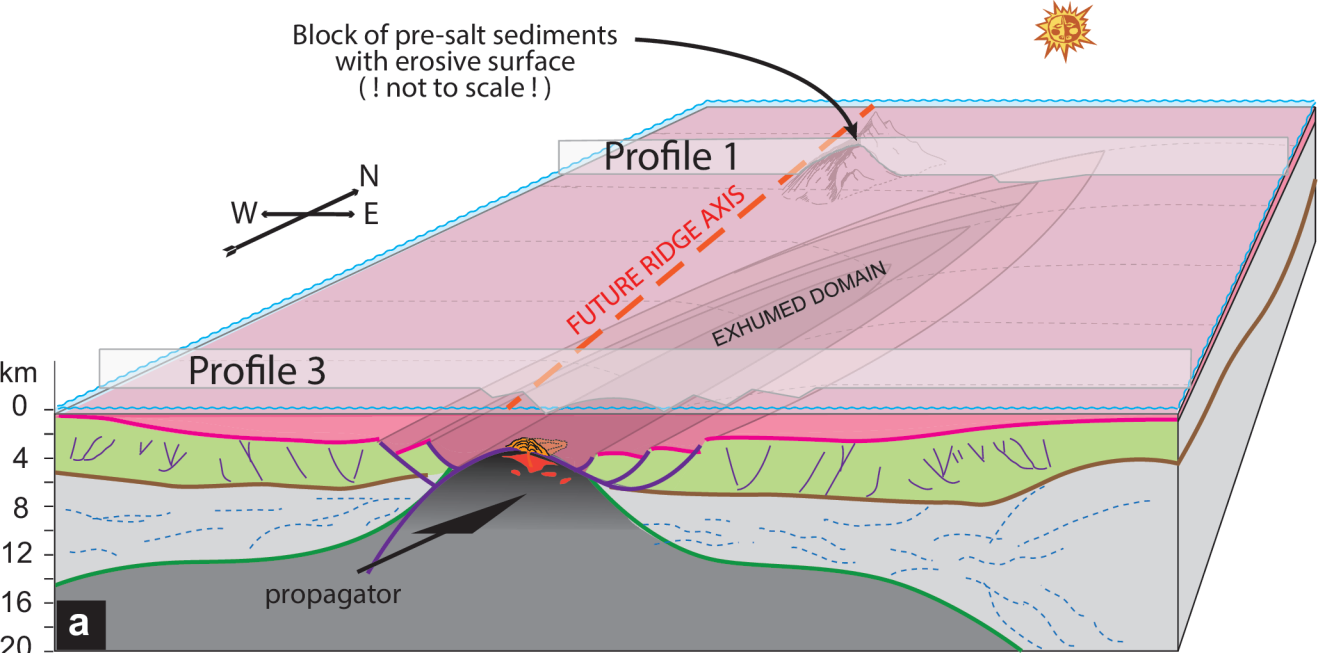
- Post-rift sediments
- Salt
- Pre-salt sediments
- Continental crust
- Oceanic crust

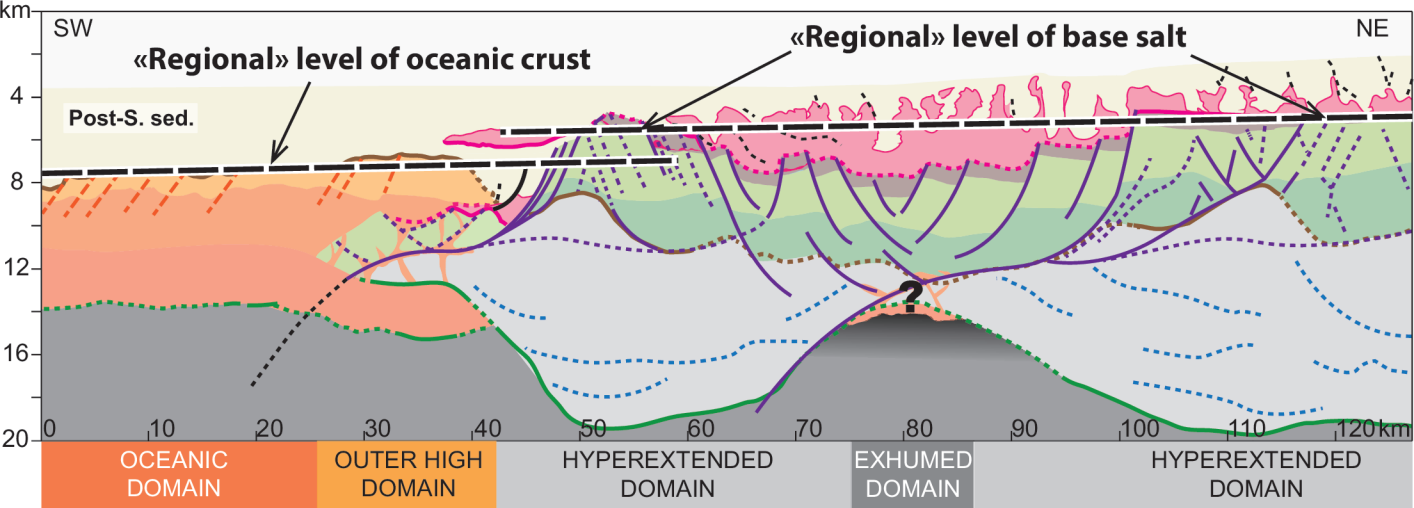
- Extrusive magmatism - Basalts
- Dikes - Sheeted dike
- Intrusive magmatism - Gabbro
- Lithospheric mantle
- Serpentinization front







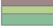


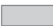


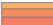

- Faults
- Unconformity
- Base salt
- Top basement
- Moho



-  Salt
-  Pre-salt sediments
-  Unconformity
-  Faults





- | | | |
|--|---|--|
|  Post-salt sediments |  Extrusive magmatism - Basalts |  Fault generation |
|  Salt |  Dikes - Sheeted dike |  Base salt |
|  Pre-salt sediments |  Intrusive magmatism - Gabbro |  Top basement |
|  Continental crust |  Lithospheric mantle |  Moho |
|  Oceanic crust |  Serpentinization front | |